Editing Transgenic DNA Components by Inducible Gene Replacement in *Drosophila melanogaster*

Chun-Chieh Lin and Christopher J. Potter[1]
The Solomon H. Snyder Department of Neuroscience, Johns Hopkins University School of Medicine, Baltimore, Maryland 21205

ABSTRACT Gene conversions occur when genomic double-strand DNA breaks (DSBs) trigger unidirectional transfer of genetic material from a homologous template sequence. Exogenous or mutated sequence can be introduced through this homology-directed repair (HDR). We leveraged gene conversion to develop a method for genomic editing of existing transgenic insertions in *Drosophila melanogaster*. The clustered regularly-interspaced palindromic repeats (CRISPR)/Cas9 system is used in the **h**omology **a**ssisted **C**RISPR **k**nock-in (HACK) method to induce DSBs in a *GAL4* transgene, which is repaired by a single-genomic transgenic construct containing *GAL4* homologous sequences flanking a *T2A-QF2* cassette. With two crosses, this technique converts existing *GAL4* lines, including enhancer traps, into functional *QF2* expressing lines. We used HACK to convert the most commonly-used *GAL4* lines (labeling tissues such as neurons, fat, glia, muscle, and hemocytes) to *QF2* lines. We also identified regions of the genome that exhibited differential efficiencies of HDR. The HACK technique is robust and readily adaptable for targeting and replacement of other genomic sequences, and could be a useful approach to repurpose existing transgenes as new genetic reagents become available.

KEYWORDS gene conversion; CRISPR/Cas9; homology-directed repair; genomic engineering; updating transgenes

DOUBLE-strand DNA breaks (DSBs) in genomic DNA are potentially lethal to the cell as they are substrates for genomic rearrangements. Two major endogenous repair mechanisms exist to resolve such DNA damage. Nonhomologous end-joining (NHEJ) involves ligation of the damaged ends and often results in small insertion/deletion (indel) mutations at the site of the DSB (Lieber 2010). This causes frameshifting and the expression of mutated or nonfunctional protein. In contrast, homologous recombination (HR) uses a homologous template for repair to preserve genomic integrity. Gene conversion is one form of HR and involves unidirectional transfer of genetic material from a donor sequence to a highly homologous target (Engels *et al.* 1990; Gloor *et al.* 1991; Chen *et al.* 2007). Donors can be from the sister chromosome (allelic gene conversion) or dispersed sequences not at the same locus (ectopic gene conversion).

Current genomic engineering methods use a DSB induced at a target genomic locus to generate disrupting mutations, driven by NHEJ, or to introduce new genetic sequences, driven by homology-directed repair (HDR). Several techniques have been developed to introduce target-specific DSBs, including zinc-finger nucleases, transcription-activator-like effecter nucleases, and, most recently, clustered regularly-interspaced palindromic repeats (CRISPR) (Jinek *et al.* 2012; Doudna and Sontheimer 2014). Cas9 is the endonuclease of the type II CRISPR system and creates a DSB at genomic locations directed by a guide RNA (gRNA). The CRISPR/Cas9 system is favored for its high efficiency and ability to use a small gRNA to specifically target most genomic DNA locations (Cong *et al.* 2013; Hsu *et al.* 2013).

Genomic engineering methods for investigating biological questions are often complemented by the use of transgenic manipulations. The development of binary expression systems in *Drosophila* has allowed for the precise manipulation of specific cell types. A binary expression system consists of two components: an exogenous transcription factor [*e.g.*, GAL4 (Brand and Perrimon 1993), QF (Potter *et al.* 2010; Riabinina *et al.* 2015), and LexAVP16 (Lai and Lee 2006)] that is expressed in a specific pattern, and an effecter gene under the regulatory control of the exogenous transcription factor (DNA sequences: *UAS*, *QUAS*, and *LexAOP*, respectively). Currently, two methods are used to generate most driver lines. In the first approach, enhancer trap lines are generated by random insertion of a transposable element carrying a minimal

doi: 10.1534/genetics.116.191783
Manuscript received May 19, 2016; accepted for publication June 7, 2016; published Early Online June 22, 2016.
Supplemental material is available online at www.genetics.org/lookup/suppl/doi:10.1534/genetics.116.191783/-/DC1.
[1]Corresponding author: 434 Rangos Bldg., 855 N. Wolfe St., Baltimore, MD 21205. E-mail: cpotter@jhmi.edu

promoter and the exogenous transcription factor (*e.g.*, *GAL4*) into the genome (Brand and Perrimon 1993; Ito *et al.* 1997; Yoshihara and Ito 2000). The transgene is able to capture expression patterns induced by its inserted genomic location. This is a useful approach, as it does not require the enhancer regions driving expression to be characterized, nor that these enhancer regions be within a small genomic region. However, generating enhancer trap lines can require labor-intensive *in vivo* screens to identify expression patterns of interest. A second systematic approach uses defined sizes of 5′ regulatory regions to generate transgenic binary expression libraries. The Janelia Research GAL4 collection uses short elements of genomic DNA (~3 kb) as potential enhancer elements, and inserts expression constructs at the same site in the genome by PhiC31 integration [*GMR-GAL4* lines (Pfeiffer *et al.* 2008; Jenett *et al.* 2012)]. The expression patterns of the GMR lines are well defined (Jenett *et al.* 2012). To date, >10,000 enhancer trap GAL4 lines and 7000 GMR-GAL4 lines have been generated. Many GAL4 enhancer traps are recognized as representatives for different tissues (*e.g.*, *elav-GAL4* is a marker for neurons and *repo-GAL4* is a marker for glia).

Complex tissues, such as the nervous system, often require the use of two binary expression systems to drive intersectional expression patterns or to examine interactions between cells (Potter *et al.* 2010). However, unlike GAL4, relatively few QF or LexAVP16 lines have been generated. Several methods have been developed to swap transcription factor drivers between transgenic binary expression systems. However, this requires either *de novo* generation of new driver lines [integrase swappable *in vivo* targeting element (InSITE)] (Gohl *et al.* 2011) or PhiC31-induced insertion of a transcription factor cassette into an existing minos mediated integration **c**assette (MiMIC) genomic insertion (Venken *et al.* 2011; Diao *et al.* 2015; Gnerer *et al.* 2015).

Here, we developed a method that converts existing transgenic *GAL4* lines into *QF2* lines with two simple genetic crosses. This method uses the CRISPR/Cas9 system to induce DSBs in transgenic GAL4, and HDR to drive conversion of GAL4 into a QF2-expressing line through the use of a single transgenic donor cassette in the genome. A total of >20 commonly-requested GAL4 lines (*e.g.*, *tubP-GAL4*, *elav-GAL4*, *repo-GAL4*, *D42-GAL4*, and *Mef2-GAL4*) distributed across the genome were successfully converted into *QF2* lines. The expression patterns of the converted lines ranged from pancellular, neuron, glia, muscle, hemocyte, to adipose tissue. The *QF2* donor and the *GAL4* target could be either on the same or different chromosomes (*trans*-chromosomal). We found that conversion frequency was influenced by the chromosomal locations and the relative orientations of donor and target. Targets at some cytological locations exhibited generally high conversion rates ("hot" spots), while others were rarely converted ("cold" spots). Our method introduces a quick and easy approach to target existing GAL4 lines, and eliminates the necessity for expensive injections or time-consuming repetitive cloning. The approach can be adapted for similar targeting or conversion of other genetic elements (such as *GAL80*, *split-GAL4*, *LexA*, *FLPase*, and *GFP*). We named this method **h**omology **a**ssisted **C**RISPR **k**nock-in or HACK.

Materials and Methods

Construction of the QF2^{G4H} HACK vector

To generate a versatile construct with multiple synthetic components, we *de novo* designed the donor vector for DNA synthesis (DNA2.0, Newark, CA). The construct contains 5′ and 3′ *P*-element sequences, *attB* sequence, *T2A*, origin of replication, and ampicillin resistance sequence. *3xP3-RFP* flanked with *LoxP* sites was PCR amplified from *pXL-BACII-LoxP-3xP-RFP-LoxP* (Addgene #26852; C. J. Potter, unpublished vector) to serve as the marker for the construct. *QF2* and *hsp70 terminator* were PCR amplified from *pQF2WB* (Addgene #61312; Riabinina *et al.* 2015). The two empty tandem gRNAs driven by U6:1 and U6:3 promoters were PCR amplified from *pCFD4-U6:1_U6:3* (Addgene #49411; Port *et al.* 2014). We named the backbone construct *pHACK-QF2* (Addgene #80274).

The manufacture of the *QF2^{G4H}* HACK donor construct required two steps. First was the selection of the gRNAs to generate DSBs in *GAL4*. Two gRNAs targeting the *GAL4* middle region were designed through an online program (http://flycrispr.molbio.wisc.edu/tools) (Gratz *et al.* 2014) and cloned into *pHACK-QF2* through *Bbs*I sites. We targeted 120 bp of sequence in the middle of GAL4. Selection criteria for the gRNA included no off-targets in the *Drosophila* genome and generation of roughly equal 5′ and 3′ homology sequences. Next, 5′ truncated homology *GAL4* (1182 bp) and 3′ truncated homology *GAL4* (1368 bp) sequences not including the gRNA targeted sequences were cloned through the *Mlu*I and *Spe*I sites. Flanking *FRT* sites between 5′ and 3′ homology arms and one *I-SceI* site upstream of the 5′ homology arm were included in case the donor cassette needed to be excised and linearized for efficient conversion (Supplemental Material, Figure S2) (Rong and Golic 2000). This proved unnecessary and was not experimentally tested for conversion. The final construct was named *pHACK-G4 > QF2* (Addgene #80275). The constructs were sent to Rainbow Transgenic Flies (Camarillo, CA) for injections for random *P*-element insertion or PhiC-31 site-specific integration at the *attP2* site. In-Fusion cloning was used for all the cloning steps (Clontech Laboratories). The *attP2 QF2^{G4H}* donor line was verified to integrate correctly into the *attP2* locus by using primers annealing to the genomic DNA sequence upstream of P2 and the other to the donor sequence (Figure S7D).

gRNA candidates used to target GAL4 sequence (PAM sequence underlined) (http://flycrispr.molbio.wisc.edu/tools):

G4_gRNA1 GATGTGCAGCGTACCACAACAGG
G4_gRNA2 TGTATTCTGAGAAAGCTGGATGG

gRNA primers to clone into pHACK-QF2:

G4_gRNA-FOR TCCGGGTGAACTTCGATGTGCAGCGTACCA
CAACGTTTTAGAGCTAGAAATAGCAAGTTA

G4_gRNA-REV TTCTAGCTCTAAAACTCCAGCTTTCTCAGAATACACGACGTTAAATTGAAAATAGGTC

Primers for 5′ homology arm (5′ homology was cloned into pHACK-QF2 through MluI site and synthetic I-SceI and FRT sequence was added into BglII site):

H1-*Bgl*II-*Bam*HI-FOR CCCTTACGTAACGCGagatctggatccATGAAGCTACTGTCTTCTATCGAA

H1-*Bam*HI-REV CGCGGCCCTCACGCGaggatccAAGCAGGGACAATTGGATCT

H1-I-SceI-FRT ACGTAACGCGAGATCtGAAGTTCCTATTCTCTAGAAAGTATAGGAACTTCTAGGGATAACAGGGTAATaGATCTGGATCCATGA

Primers designed for 3′ homology arm (3′ homology with FRT sequence in the reverse primer was cloned into pHACK-QF2 through SpeI site):

H2-*Spe*I-FOR GTTATAGATCACTAGtCATGGCATCATTGAAACAG

H2-*Spe*I-FRT-REV AATTCAGATCACTAGAAGTTCCTATACTTTCTAGAGAATAGGAACTTCactagtCTATTACTCTTTTTTTGGGTTTG

PCR primers used for verification of HDR and indel mutation:

pGaw2 CAGATAGATTGGCTTCAGTGGAGACTG

GAL4-mdg3_genomic_FOR1 GCGTTTGGAATCACTACAGGG

GAL4_FOR2 GCACTCACCGACGCTAATGATG

PCR verification of the location of pHACK_G4 > QF2 at the P2 site:

A2_3L_REV CTCTTTGCAAGGCATTACATCTG

Pry#4 CAATCATATCGCTGTCTCACTCA

The Cas9 gRNAs directed highly efficient targeting of *GAL4* sequences (Figure S7 and Figure S8). The gRNAs were chosen using the "high stringency" algorithm to have no predicted off-targets in the *Drosophila* genome (http://tools.flycrispr.molbio.wisc.edu/targetFinder/index.php) (Gratz *et al.* 2014). However, the "maximum stringency" algorithm identified two predicted off-target sites for gRNA1, and three predicted off-target sites for gRNA2. We examined if these predicted off-target sites contained HACK-induced mutations by PCR amplifying the genomic DNA of two fly stocks containing Cas9 endonuclease and gRNAs combined for at least six generations [*Act5C-Cas9*; $QF2^{G4\text{-}HACK}$ *(57C1)* and *Act5C-Cas9*; *;* $QF2^{G4\text{-}HACK}$ *(70F4)*]. This would allow sufficient opportunities for any Cas9/gRNA-mediated indel mutations to accumulate in germline or somatic tissues. The sizes of the PCR products were indistinguishable from those of the control (*Act5C-Cas9*) (Figure S11). Furthermore, sequencing of the PCR products revealed no mutations (n = 10). These results suggest that endogenous genomic loci are unlikely to be targeted by *GAL4* gRNAs used by the HACK method.

Primers for potential off-target sites generated by gRNA1:

gRNA1_OT1F AACAACCCATCAGGACGAGC

gRNA1_OT1R AAAACGGCTGGCTTAGTTGC

gRNA1_OT2F TTGATCGTTTGGGTTTGTGC

gRNA1_OT2R GCTCTTGCACCCAGGAAAAG

Primers for potential off-target sites generated by gRNA2:

gRNA2_OT1F TCGCTCATGGTAAATGGTGC

gRNA2_OT1R TTAACGGCATGATCCTGTGC

gRNA2_OT2F ATGAGACTAGCCGAAAGGCG

gRNA2_OT2R TGGGCCTCTTCAATGTTTCC

gRNA2_OT3F TCATTTCGCAAGGATTGCAG

gRNA2_OT3R AAGCTGCGGATTTATGGGTG

The *pHACK_G4 > QF2* insertion at the *attP2* site by PhiC31 integrate is in the opposite orientation of *GMR-GAL4* lines inserted at *attP2* as generated using the *pBPGUw* vector (Addgene #17575; Figure 5C) (Pfeiffer *et al.* 2008). To address this, we used the *pBPGUw* vector as a backbone to generate a compatible HACK_G4 > QF2 plasmid. The *pHACK_QF2* vector was digested with *Sna*BI and *Pac*I followed by ligation to the *pBPGUw* backbone amplified by PCR from *pBPGUw*. The ampicillin resistance site and bacterial origin of replication might potentially affect HDR accuracy; therefore, this vector region was flanked by *mFRT71* sites for removal by mFLP5 if necessary (Hadjieconomou *et al.* 2011). The final construct was named *pBPGUw_HACK_QF2* (Addgene #80276). We cloned *GAL4* 5′ and 3′ homology arms and gRNAs as described above (*pBPGUw_HACK_G4 > QF2*, Addgene #80277; Figure S2D).

Primers to PCR amplify the backbone from pBPGUw:

pBPGUw-FOR TAATGCGTATGCTTAattaaTATGTTCGGCTTGTCGACATG

pBPGUw-REV CAGATCTCGCGTTACgtaCTTGAAGACGAAAGGGCCTC

Primers to insert mFRT71 at the SnaBI site:

TTCGTCTTCAAGTACGAAGTTTCTATACTTTCTAGAGAATAGAAACTTCtacGTAACGCGAGATCTG

Primers to insert mFRT71 at the PciI site:

GTCGACGGTAACATGtGAAGTTTCTATACTTTCTAGAGAATAGAAACTTCCATGTGAGCAAAAGG

Drosophila genetics

The fly stocks used in the study are *10xQUAS-6xGFP* (BS#52264) (Shearin *et al.* 2014), *5xUAS-mtdt-3HA* (Potter *et al.* 2010), *5xQUAS-nucLacZ* (BS#30006) (Potter *et al.*

Table 1 GAL4 lines converted to QF2 lines using the HACK method

GAL4 line	Expression pattern	BS#	Chr.	Note	QF2 line
Alrm-GAL4	Glial subset		III		Alrm-QF2^{G4H}
D42-GAL4	Motor neurons	8816	III	ET	D42-QF2^{G4H}
elav-GAL4	Pan-neuronal	458	*X*	ET	elav-QF2^{G4H}
GH146-GAL4	Olfactory PNs	30026	II	ET	GH146-QF2^{G4H}
Hml-GAL4	Hemocytes	30139	II		Hml-QF2^{G4H}
Mef2-GAL4	Pan-muscle	27390	III		Mef2-QF2^{G4H}
NP2222-GAL4	Glial subset	112830	II	ET	NP2222-QF2^{G4H}
NP2631-GAL4	MB subset	104266	II	ET	NP2631-QF2^{G4H}
OK107-GAL4	Pan-MB	106098	IV	ET	OK107-QF2^{G4H}
OK371-GAL4	vGlut neurons	26160	II	ET	OK371-QF2^{G4H}
Pebbled-Gal4	Pan-ORN, GN	Sweeney (2007)	*X*	ET	Pebbled-QF2^{G4H}
Ppk-GAL4	Type IV MD neurons	32079	III		Ppk-QF2^{G4H}
r4-GAL4	Adipose tissue	33832	III		r4-QF2^{G4H}
repo-GAL4	Pan-glial	7415	III	ET	repo-QF2^{G4H}
tubP-GAL4	Pan-cellular	5138	III		tubP-QF2^{G4H}

BS, Bloomington Stock; Chr., chromosome; ET, enhancer trap; PN, projection neuron; MB, mushroom body; vGlut, ventrolateral glutamatergic; ORN, olfactory receptor neuron; GN, gustatory neuron; MD, multidendritic.

2010), *5xUAS-GFPnls* (BS#4775), *Act5C-Cas9* (BS#54590) (Port *et al.* 2014), *Vas-Cas9* (BS#51323 on *X* chromosome and BS#51324 on third chromosome) (Gratz *et al.* 2013), and *Cre^{y+1B}* (BS#766) (Siegal and Hartl 1996). The specific *GAL4* lines from Bloomington *Drosophila* Stock Center are listed in Table 1 and Table 2.

Genetic crosses in the study are summarized in Figure 2B. In short, the parental cross combines target *GAL4* lines to *QF2^{G4H}* donor stocks that include *Act5C-Cas9* or *vasa-Cas9* on the *X* chromosome. Next, for F_1 crosses, four pairs of single male to double balancer virgin females vials (3–4 females/vial) were established for each genotype. Only F_2 male progeny were examined under light and fluorescence microscope (see below for detailed description of the setup) for w^+ and *red fluorescent protein* (*RFP*)+ eye markers. Male flies were examined between day 10 and 18 of the F_1 crosses. Typically, each vial gave rise to ~20 *w*+ and ~20 *RFP*+ male flies. The candidate HACKed flies (w^+ and *RFP*+) were further examined by crossing to reporter lines (*10xQUAS-6xGFP*) (Shearin *et al.* 2014). The *3xP3-RFP* marker can be removed by crossing to *Cre^{y+1B}* flies (Siegal and Hartl 1996). All the crosses were maintained in a 25° incubator to ensure precise timing of the life cycle.

Fluorescence microscope setup

For adult images, a Carl Zeiss (Thornwood, NY) Discovery V8 SteREO microscope equipped with Achromat S 1.0× FWD 63-mm objective and illuminated with X-Cite 120Q excitation light source was used. Images could be detected through eyepieces or directed to a charge-coupled device camera (Jenoptik ProgRes MF cool) for real time image acquisition (ProgRes Mac Capture 2.7.6). A microscope filter shield (Nightsea, #SFA-LFS-GR) was used to protect against strong reflection of green excitation light from the CO_2 pad while screening for RFP+ flies.

Acj6-GAL4 and GH146-QF2 colabeling experiment

To eliminate the olfactory neuron innervations in the antennal lobe from *Acj6-GAL4*, the antennae were removed 6 days before brain dissection for antennal nerve degeneration.

Nervous system dissection and immunohistochemistry

Dissection of the adult nervous system was performed as described previously (Potter *et al.* 2010). In short, brains and ventral nerve cords of second and third instar larvae or 4- to 6-day-old flies were dissected in 1× PBS solution and then fixed in 4% paraformaldehyde (dissolved in PBS with 0.3% Triton X-100) for 15 min. Fixation and washes were done at room temperature. Fixed tissues were washed three times with PBS + 0.1% Tween-20 (PBT) before incubating in PBT twice for 20 min. A 5% normal goat serum dissolved in PBT blocking solution was used to wash tissues for 30 min. Next, the tissues were placed in primary antibody mixes for 1–2 days at 4° followed by two 20 min PBT washes. The tissues were placed in secondary antibody mixes for 1 day in the dark at 4°. The following day the tissues were washed in PBT for 20 min and placed in mounting solution (Slow Fade Gold) for at least 1 hr before imaging. All wash steps were performed at room temperature.

For the nuclear colocalization experiments of *TubP* and *repo* drivers, the primary antibodies included preabsorbed rabbit anti-LacZ (1:50, Cat#559761; MP Biochemicals) and chicken anti-GFP (1:1000, #GFP1020; Aves Labs) antibodies. Secondary antibodies were Alexa 649 anti-rabbit (1:200, #DI-1649; Vector Laboratories, Burlingame, CA) and Alexa 488 anti-chicken (1:200, #A11039; Invitrogen, Carlsbad, CA). To label the cell nucleus, nervous tissues were incubated with DAPI (1:1000 dissolved in PBT, #21094; Invitrogen) for 10 min at room temperature after the secondary antibody wash step.

To enhance GFP signals, primary antibodies used in the study were rabbit anti-GFP (1:250, #A11122; Life Technologies), chicken anti-GFP (1:1000, #GFP1020; Aves Labs), and rat anti-mCD8 (1:250, MCD0800, in the experiments using mCD8:GFP as the reporter; Invitrogen). Secondary antibodies were Alexa 488 anti-rabbit (1:200, #A11034; Invitrogen), Alexa 488 anti-chicken (1:200, #A11039; Invitrogen) and Alexa 488 anti-rat (1:200, #A11006; Invitrogen). For mtdt-3HA, we used rat anti-HA (1:250, #11867423001; Hofmann La Roche, Nutley, NJ) as the primary antibody and Cy3 anti-rat (1:200, #112-165-167;

Table 2 *GMR-GAL4* lines converted to *QF2* lines using the HACK method

GAL4 line[a]	Neuronal expression pattern	BS#	QF2 line
GMR57C10-GAL4	Pan-neuronal	39171	GMR57C10-QF2^{G4H}
GMR58E02-GAL4	Dopaminergic subset	41347	GMR58E02-QF2^{G4H}
GMR10A06-GAL4	Olfactory receptor neurons	48237	GMR10A06-QF2^{G4H}
GMR20A02-GAL4	DN1 central body neurons	48870	GMR20A02-QF2^{G4H}
GMR24C12-GAL4	Olfactory interneurons	49076	GMR24C12-QF2^{G4H}
GMR71G10-GAL4	Mushroom body subset	39604	GMR71G10-QF2^{G4H}
GMR82G02-GAL4	Mushroom body subset	40339	GMR82G02-QF2^{G4H}
GMR16A06-GAL4	Mushroom body subset	48709	GMR16A06-QF2^{G4H}

[a] *GMR-GAL4* lines inserted at *attP2* on third chromosome (68A4).

Jackson ImmunoResearch) as the secondary antibody. If 3xP3-RFP was not removed, we used Alexa 633 anti-rat (1:200, #A21094; Invitrogen) as secondary the antibody. To visualize the structure of the nervous system, mouse anti-nc82 (1:25; Developmental Studies Hybridoma Bank) was used as the primary antibody and Alexa 647 (1:200, Z25008; Life Technologies) or Cy3 anti-mouse (1:200, 115-165-166; Jackson Immuno Research) as the secondary antibody.

Confocal imaging and image processing

Confocal images were taken on a Carl Zeiss LSM 710 confocal microscope equipped with 10× (Fluar 10×/0.5, Carl Zeiss) and 40× (Plan-Apochromat 40×/1.3 oil DIC, Carl Zeiss) objectives. Zen 2012 software was used for image acquisition. For illustration purposes, Z-stack images were collapsed onto a single image by ImageJ using maximum-intensity projection and pseudocolored into different acquisition channels using a red-green-blue plug-in.

Data availability

Drosophila lines are available at Bloomington *Drosophila* Stock Center or upon request. Plasmid constructs are available at Addgene or upon request.

Results

Editing DNA sequences by targeted gene conversion

We describe a genomic engineering process that drives gene conversion using a single DNA donor template (Figure 1). DNA donors are integrated into the genome by random *P*-element insertions. The donor consists of two components: homology sequences for repair searching and genetic material for HDR-mediated insertion. When a DSB is introduced at the target sequence, the donor is employed as a template for DNA repair through HDR and the DNA of interest is also incorporated. The donor can then be separated from the target by genetic crosses. The final result is generation of a target containing the DNA of interest (Figure 1, dashed red arrow, and Figure S1).

HACK converts GAL4 transgenes into QF2

We employed an artificial gene conversion method to target the *GAL4* sequence for insertion of donor DNA (Figure 2). Given the need for well-defined transactivators of other binary expression systems, we chose to design DNA sequences that would convert *GAL4* into a different binary expression transactivator: *QF2*. *GAL4* homology arms are required for repair searching in HDR and will remain in the genome after conversion. To generate a functional QF2-expressing line, the donor DNA sequence inserted is a *T2A-QF2* coding cassette in frame with the targeted *GAL4* (Figure 2A and Figure S2). T2A is a ribosomal skipping sequence that allows polycistronic protein translation from the same RNA transcript (Diao and White 2012). Thus, the genomic enhancer/promoter would drive 5′ truncated GAL4 and QF2 proteins (Figure 2A). This converts a *GAL4* transgene into a *QF2* transgene (Figure 2A).

To monitor a successful HDR-mediated insertion of the desired sequence, the *QF2* donor also contains an eye marker for transgenic screening (*3xP3-RFP*) (Figure 2A). Outside the homologous target regions are RNA polymerase III-dependent U6 promoters used to transcribe Cas9 gRNAs targeting the middle region of the *GAL4* sequence. In the presence of Cas9 protein driven by *Act5C* or *Vasa* promoters (Ren *et al.* 2013; Gratz *et al.* 2014), two independent DSBs will be generated in the *GAL4* sequence. The damaged DNA could be repaired by either NHEJ or HDR. In the case of HDR, the damaged double-stranded DNA associates with a repair protein complex that initiates a search for homologous sequences in the genome as a template for repair (Bernstein and Rothstein 2009). If the exogenous *QF2* donor is used then the *T2A-QF2* and *3xP3-RFP* are inserted into the *GAL4* sequence (Figure 2A). Successful HACK events can be screened by identifying animals that express RFP in the eyes (Figure 2B and Figure S1). The *3xP3-RFP* is flanked by loxP sites and can be subsequently removed with Cre recombinase (Figure S3) (Siegal and Hartl 1996).

Crossing scheme and nomenclature of HACK system

Through genetic crosses, target (*X-GAL4*), donor (*QF2^{G4HACK}*), and *Act5C-Cas9* (or *Vas-Cas9*) were combined in the same animal (Figure 2B, parental cross). The F_1 male progeny were crossed to wild type or balancer flies. Since *Drosophila* males do not undergo chromosomal recombination during meiosis, the F_2 male will contain either the *w+* or *RFP* marker, which indicates *GAL4* and *QF2^{G4HACK}* transgenes, respectively. F_2 males containing double markers (*w$^+$* and *RFP*) indicate successful HDR-mediated incorporation of *T2A-QF2* and *3xP3-RFP* into the *GAL4* sequence (Figure 2B and Figure S1). Due to positional

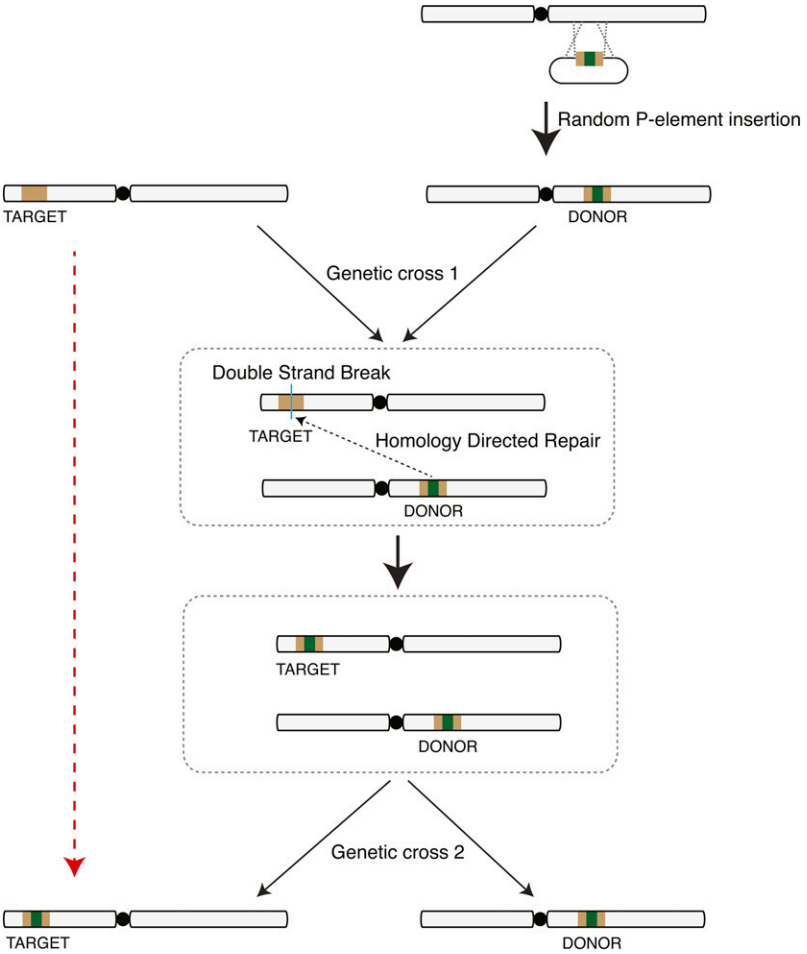

Figure 1 Schematic outlining gene conversion using homology-directed repair from an integrated transgene. A donor plasmid consisting of a core cassette carrying the DNA of interest for incorporation (green) flanked by target homology arms (brown) is randomly inserted into the genome by *P*-element transposition. A genetic cross brings the target and donor together into the same cell. A DSB is induced in the target DNA to trigger HDR-mediated insertion of the DNA of interest into the target. A second genetic cross segregates the converted target and donor insertions. The final result (red dashed arrow) is insertion of donor sequence into the target site.

effects (Levis *et al.* 1985), the *GAL4*-to-*QF2* converted flies might demonstrate different patterns and levels of RFP expression compared to the *HACK* donor. Successfully HACKed lines were named *X-QF2*^{G4HACK} (or *X-QF2*^{G4H} for short). This establishes a nomenclature *X-Y*^{ZHACK} in which *X* refers to the original enhancer/promoter locus, *Y* refers to the introduced DNA element, *Z* refers to the replaced DNA element, and HACK indicates the reagent was generated using the HACK method.

HACK conversion with a ubiquitously-expressed GAL4 line

Tubulin is a major component of the eukaryotic cytoskeleton and as such the tubulin promoter can drive ubiquitous GAL4 as detected by a GFP reporter (*TubP-GAL4* > *UAS-mCD8:GFP*). We used *QF2*^{G4H} at cytological location 64B5 to HACK the *TubP-GAL4* at 79A2 (Figure 2C). Of the 128 F_2 w^+ males screened, 3 of them exhibited both w^+ and *RFP* eye markers (Figure 2D). We calculated the efficiency of HACK conversion as 3/128 (2.3%) (see Figure S1 for definition of conversion rate). Note, this involved setting up four single male F_1 crosses (Figure 2B), yet a single male F_1 cross may have been sufficient to identify a conversion event. We verified the *TubP-QF2*^{G4H} lines by genomic sequencing and expression pattern comparison (Figure 2E and Figure S3). All three *TubP-QF2*^{G4H} lines drive GFP expression under control of *QUAS*, and no mtdt-3HA signal was detected when crossed to *UAS-mdt-3HA* (*TubP-QF2*^{G4H} > *10XQUAS-6xGFP*, *5XUAS-mtdt-3HA*) (Figure 2E, Figure S3, C and D). Similarly, *TubP-QF2*^{G4H} failed to drive expression in salivary glands from a *UAS-GFPnls* reporter (Figure S3E). Nuclear reporters driven by *TubP-GAL4* and *TubP-QF2*^{G4H} colocalized in the dissected larval brain tissue (Figure 2F). These data suggested that *TubP-QF2*^{G4H} recapitulated the expression pattern of the original *TubP-GAL4* line.

The *X-QF2*^{G4H} expresses a 5′ truncated GAL4 that contains the GAL4 DNA-binding domain and could potentially bind to *UAS* sequences, which might interfere with the function of other GAL4 transgenes. To address this, we examined the effects of *X-QF2*^{G4H} coexpressed with *Y-GAL4* using olfactory projection neuron lines that target well-characterized subsets of neuronal populations. We first generated *GH146-QF2*^{G4H} from *GH146-GAL4* (Figure S4, A and B). *GH146* drives expression in ~150 well-defined projection neurons situated around the antennal lobes (Jefferis *et al.* 2007). The *Acj6-GAL4* expression pattern partially overlaps with *GH146* in anterodorsal projection neurons. When combined (*Acj6-GAL4* > *5XUAS-mtdt-3HA*, *GH146-QF2*^{G4H}>*10XQUAS-6xGFP*) (Komiyama *et al.* 2004), *GH146-QF2*^{G4H} does not appear to affect the *UAS-geneX* signal of Acj6 positive neurons (Figure S4C), suggesting that the truncated GAL4 protein is

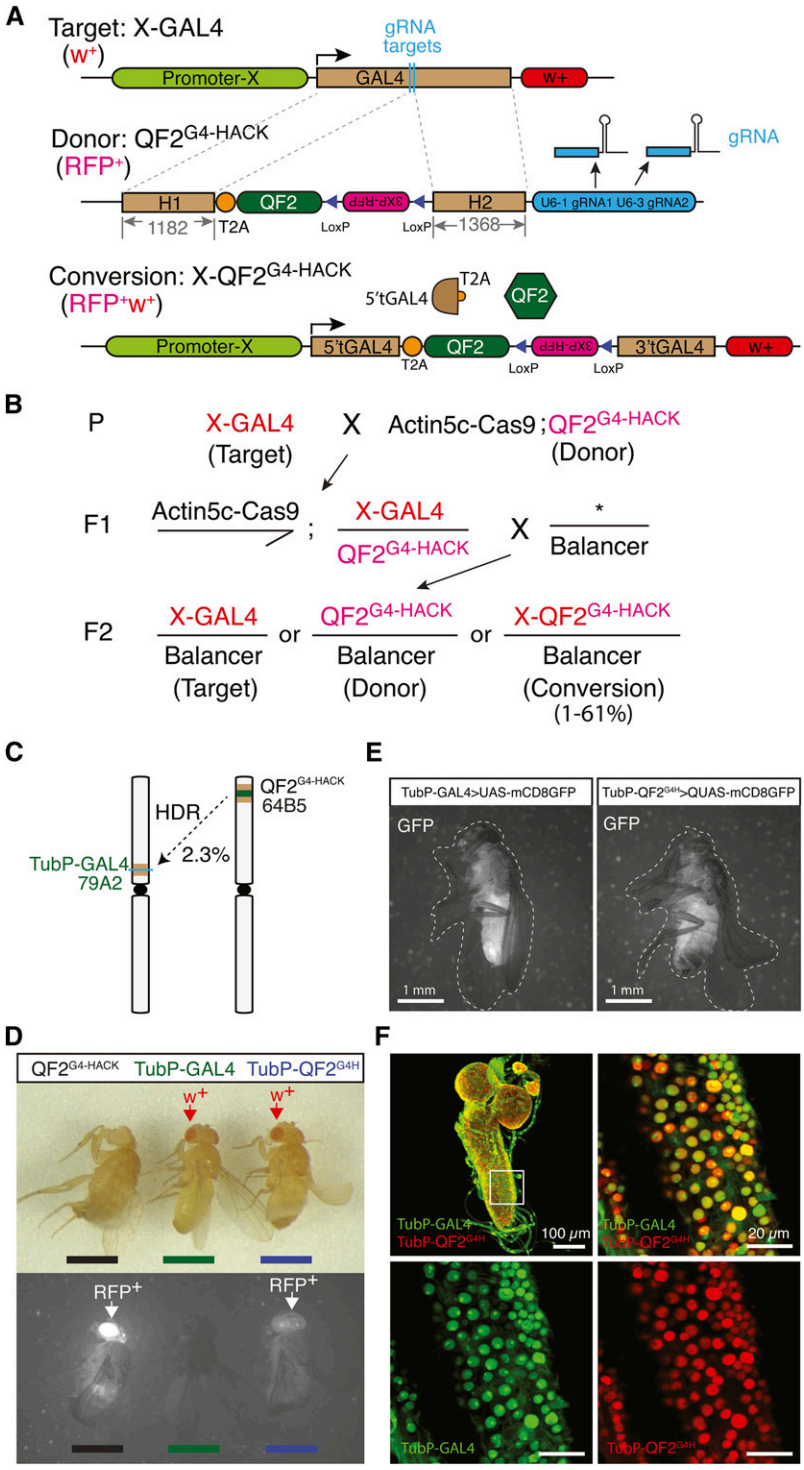

Figure 2 HACK can be used to convert *GAL4* lines into *QF2* lines. (A) Genetic reagents for *GAL4* to *QF2* HACKing. The target is a *GAL4* transgenic line (*X-GAL4*). The *QF2*$^{G4\text{-}HACK}$ donor consists of 5′ and 3′ GAL4 homology arms flanking an in-coding frame *T2A-QF2* and a *3xP3-RFP* eye marker. Outside the *GAL4* homology arms are *U6:1* and *U6:3* promoters used to express two independent gRNAs that target *GAL4* for DSBs in the presence of the Cas9 protein. After conversion, the *X-QF2*$^{G4\text{-}HACK}$ line contains the *T2A-QF2* cassette and the *3xP3-RFP* marker. The *U6*-gRNAs are not included in the converted target. (B) Converting *GAL4* lines to *QF2* lines using the HACK system involves two genetic crosses. The success rate depends on both the target and donor lines but ranges from 0 to 60%. (C) *TubP-GAL4* (79A2) was HACKed using a *TubP-QF2*^{G4H} (64B5) insertion. (D) The donor (*QF2*^{G4H}) and target (*TubP-GAL4*) contain a single eye marker, *RFP* or *w*$^{+}$, respectively. A successfully HACKed line (*TubP-QF2*^{G4H}) is double positive for the eye markers (*RFP* and *w*$^{+}$). (E) The pan-tissue expression pattern of *TubP-QF2*^{G4H} is consistent with that of *TubP-GAL4*. Bar, 1 mm. (F) Second instar larvae labeled by nuclear-localized reporters for both *TubP-GAL4* (green) and *TubP-QF2*^{G4H} (red). Note that GFPnls and nucLacZ show different subnuclear localization. GFPnls is found more concentrated in the nucleolus while nucLacZ is excluded from the nucleolus. Genotype: *TubP-GAL4>UAS-nucGFP, TubP-QF2*^{G4H} *> QUAS-nucLacZ*. Bar, 100 μm (left top image) and 20 μm (zoomed-in images). Left top image is 118 μm Z stack and the other three are 3.84 μm stacks.

either nonfunctional or possibly degraded. In addition, the *GH146-QF2*^{G4H} line more closely mimics the original *GH146-GAL4* enhancer trap expression pattern than an enhancer-cloned transgenic *GH146-QF2* line (Figure S4D).

Establishing a collection of QF2^{G4H} *donor lines throughout the genome*

Previous studies in human somatic cells have found that homologous chromosomes make contact at the sites of DSBs (Gandhi *et al.* 2012). Furthermore, in yeast, the efficiency of repair after DSB is correlated with the contact frequency of the donor and damaged sites (Lee *et al.* 2016). We reasoned that the locations of the target and the donor relative to each other might contribute to the success rate of HACK, with greatest efficiency when the donor and the target are in close proximity on sister chromosomes. To enable essentially any *GAL4* target to be HACKed, and to examine efficiencies of gene conversion by different donor lines, we generated a

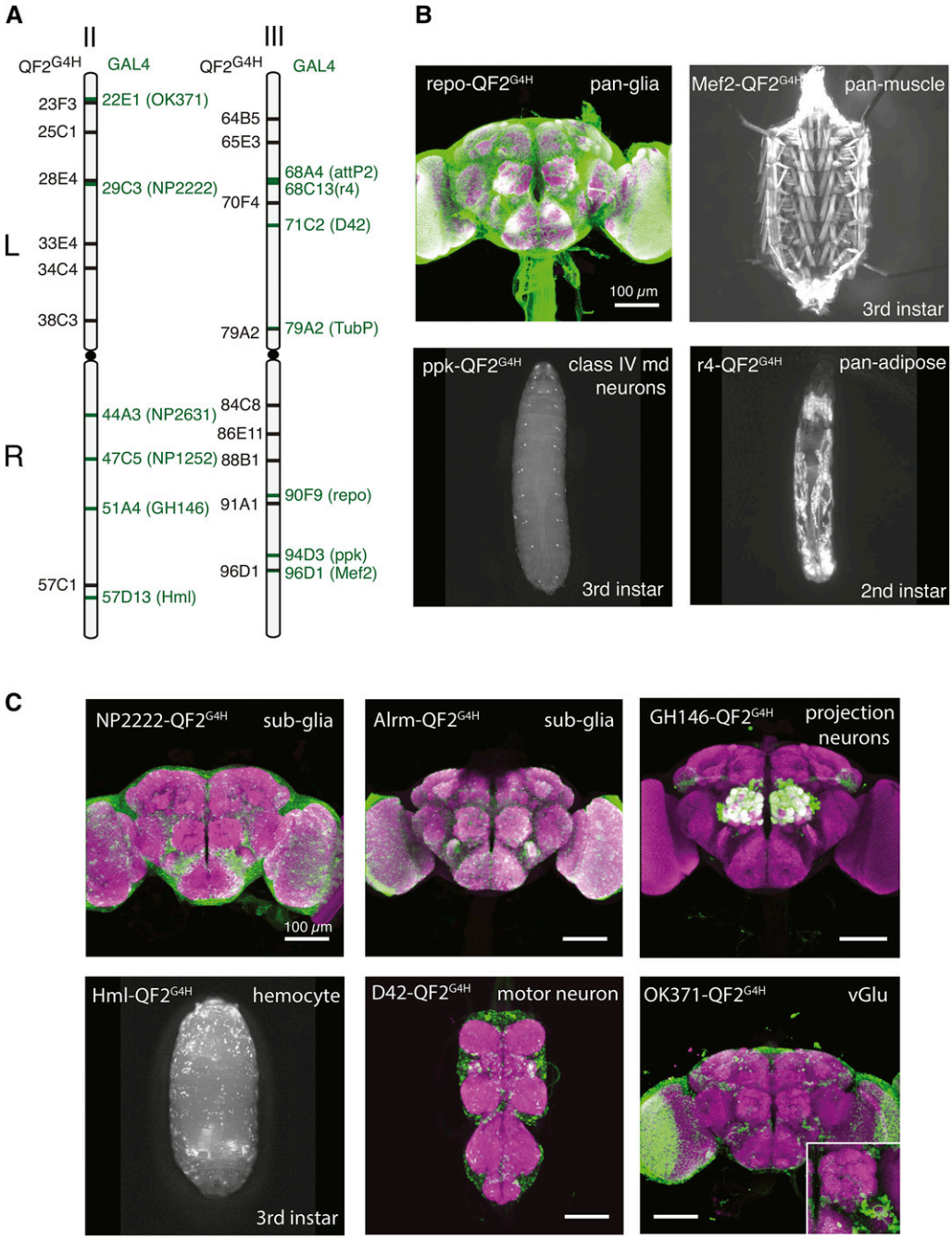

Figure 3 HACK can be applied to convert commonly-used GAL4 lines at various genomic locations. (A) Cytological locations of *QF2^{G4H}* and *GAL4* lines used in this study. The *GAL4* lines are distributed across the second and third chromosomes. (B–C) Examples of *QF2^{G4H}* lines generated by the HACK method using *GAL4* lines with (B) broad (*e.g.*, pan-glial) and (C) defined (*e.g.*, class IV multidendritic neurons) expression patterns. Purple, nc82 antibody staining; Green, GFP antibody staining. Bar, 100 μm (brain and ventral nerve cord).

QF2^{G4H} donor collection by random *P*-element transgenesis (Figure 1). A total of 7 out of 9 lines on the second chromosome and 9 out of 18 lines on the third chromosome were selected as candidate *QF2^{G4H}* donors for their fairly even distribution along the chromosomes (Figure 3A and Figure S5).

HACK is effective for the conversion of GAL4 lines inserted across the whole genome

GAL4 enhancer traps are useful reagents, yet reproducing the desired expression pattern as a transgene may be difficult to accomplish (Potter and Luo 2010). To test if HACK can be used to convert a variety of genomic locations, we targeted the most frequently requested GAL4 stocks available from the Bloomington *Drosophila* Stock Center (Table 1; Bloomington *Drosophila* Stock Center, personal communication). These GAL4 lines were systematically crossed to the *QF2^{G4H}* donor collection to generate *X-QF2^{G4H}* lines and assess conversion success rates.

Toxicity was occasionally an issue for QF constructs, but was recently solved with the introduction of QF2 (Riabinina *et al.* 2015). To further verify that high QF2 expression levels would not affect HACK efficiencies, additional pan-tissue GAL4 lines were first assayed: *repo-GAL4* (pan-glia), *Mef2-GAL4* (pan-muscle), *Hml-GAL4* (hemocyte), and *r4-GAL4*

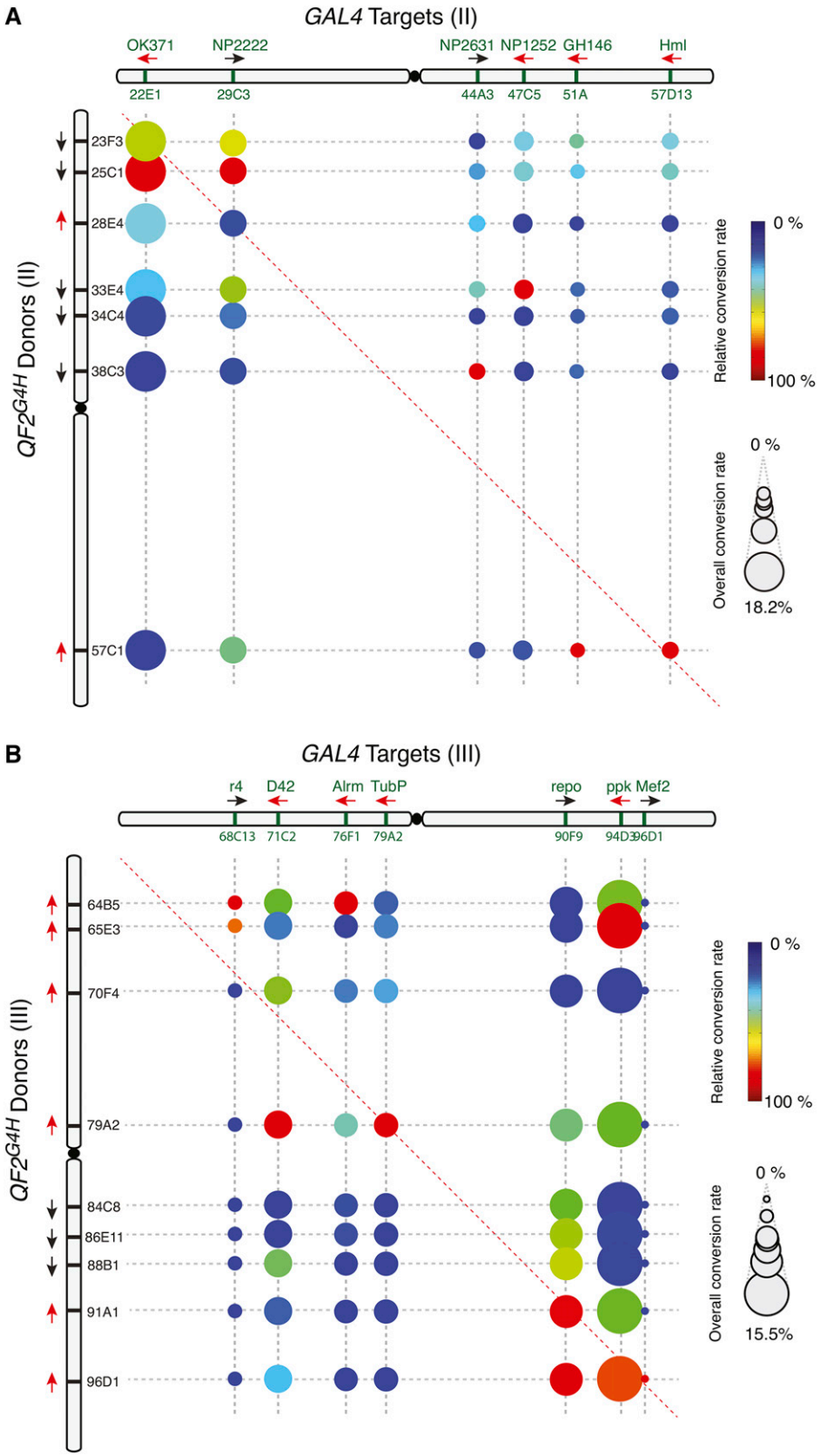

Figure 4 HACK efficiencies across the second and third chromosome. (A–B) Conversion frequencies were tested for each donor and target pair on the (A) second or (B) third chromosome. The size of the circle represents the overall conversion rate of the target GAL4 line to all tested donor lines. Larger circles represent target GAL4 sites that were easier to convert (hot spots), while smaller circles represent target GAL4 sites that demonstrated low conversions (cold spots). For example, 18.2% of all F_2 progeny of crosses from *OK371-GAL4* and all seven second chromosome donors demonstrated conversions. The color indicates the relative conversion rate of the donor normalized to the highest conversion rate for the corresponding GAL4 lines. Thus colors indicate which donor line is most efficient for driving $QF2^{G4H}$ HACK conversions for a particular *GAL4* line. For example, for *OK371-GAL4*, $QF2^{G4H}$ donor at 25C1 was the most effective (relative conversion rate 100%), and $QF2^{G4H}$ at 23F3 roughly two-thirds as effective (relative conversion rate 67%). Black and red arrows indicate the inserted transgene is in the forward and reverse orientation, respectively, relative to the reference *Drosophila* genome (Flybase R6.10).

(pan-adipose tissue). All lines were successfully converted into $QF2^{G4H}$ lines with the expected expression patterns (Figure 3). Next, we examined widely-used *GAL4* lines with defined expression patterns: *NP2222-GAL4* (glial subset), *Alrm-GAL4* (glial subset), *GH146-GAL4* (olfactory projection neurons; see above), *ppk-GAL4* (type IV multidendritic neurons), *D42-GAL4* (motor neurons), *NP2631-GAL4* (mushroom body subset), and *OK371-GAL4* (ventrolateral glutamatergic

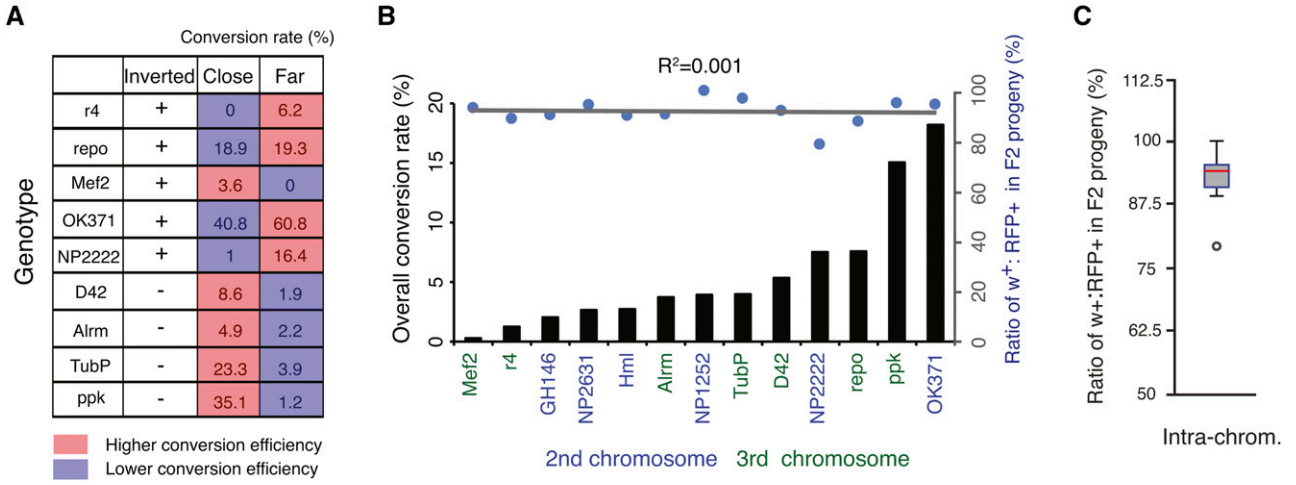

Figure 5 HACK efficiency depends on the genomic distance and orientation of target and donor and reveals hot and cold spots of homology-directed gene conversion. (A) Comparison of conversion efficiencies using close (donor and target within 0–3 cytological bands) and far (donor and target within 3–6 cytological bands) revealed relative orientations of target and donor influence HACK conversion efficiencies. (B) Overall conversion rates of the 13 GAL4 lines show >50-fold range differences (black bars) but are not correlated with a reduced fitness caused by DSB HACK events in *GAL4*, as measured by the ratio of w+ (*GAL4*+) to RFP+ ($QF2^{G4H}$) F_2 animals. (C) During the HACK process, the presence of the gRNA target sequence (*GAL4*) decreases the survival rate of flies containing *GAL4* chromosomes by 7.4% when compared to progeny lacking GAL4 target sequences. $N = 21{,}293$ flies.

neurons). We included *NP1252-GAL4* at 47C5 to test the efficiency of targeting a *GAL4* in that region. These lines were all successfully HACKed, and expression patterns driven by QF2 were consistent with those of the GAL4 lines (Figure 3, Figure S6, and Table 1). Of the 14 *GAL4* lines we tested, only 1 GAL4 line (*en2.4-GAL4* at 47F15, BS#30564) could not be HACKed after two attempts (see *Discussion*). Of the successfully HACKed flies with both eye markers, all of them exhibited consistent expression patterns as compared to the original GAL4 lines ($N > 100$).

HACK efficiency varies with different target and donor pairs

We examined all pairwise conversion efficiencies between the second chromosomal *GAL4* target and $QF2^{G4H}$ donor lines, as well as all pairwise conversion efficiencies between the third chromosomal *GAL4* target and $QF2^{G4H}$ donor lines. In general, the efficiency of gene conversion appears to relate directly to the proximity of the donor and target insertion sites in the homologous chromosomes (Figure 4, A and B). The closer a donor line is to a *GAL4* target in the homologous chromosome, the higher the efficiency of conversion. However, we observed >50-fold differences in the overall conversion rates, ranging from 0.28% for *Mef2-GAL4* to 18.2% for *OK371-GAL4* (Figure 5, A and B). Thus, some genomic regions appeared more efficient at gene conversion (hot spots) and some were more difficult to convert (cold spots).

Consistent with previous observations (Engels *et al.* 1994), the orientation of the donor and target (forward or reverse in relation to the sequenced genome) can also affect gene conversion frequency. We compared HACK frequencies of donor and target pairs that are within 3 cytological bands (close pairs) with those between 3–6 cytological bands (far pairs). When the donors and targets are in the same orientation, 4 out of 4 close pairs exhibit high conversion rates. In contrast, 4 out of 5 far pairs exhibit higher conversion when donors and targets are inverted (Figure 5A).

DSBs are potent inducers of genomic mutations and cell death. In the HACK process, the *GAL4* sequence serves as the target for Cas9 endonuclease. We examined whether HACK affects the general health of individual flies by comparing the number of observed RFP ($QF2^{G4H}$) and w+ (*X-GAL4* and $X\text{-}QF2^{G4H}$) flies in the F_2 generation (see crossing scheme in Figure 2B). Mendelian genetics predicts that *RFP*+ and w^+ F_2 progeny should be in a 1:1 ratio, and deviations from this ratio indicate fitness costs. There is a ~7.4% decrease in the number of predicted w^+ (GAL4+) progeny as compared to control RFP+ donor flies (Figure 5C, ratio = 0.926, SEM = 0.015, $n = 13$ F_1 crosses with a total of 21,293 F_2 flies). A regression curve showed no correlation between survival percentage of $GAL4^+$ flies and the HACK success rate (Figure 5B, slope = −0.004, $R^2 = 0.001$). This suggests that DSBs occur equally in all *GAL4* targets, and that the introduction of a DSB in the *GAL4* gene is a likely factor in reducing progeny fitness. Furthermore, the data suggest that differences in GAL4 conversion rates are more likely due to differences in HDR efficiencies.

Allelic genes do not necessarily lead to high conversion rates

A simple prediction would be that donors and targets at allelic sites on homologous chromosomes would demonstrate maximal gene conversion rates. In *Drosophila*, transgenes can be inserted into a specific locus using the PhiC31/attP integrase system (Groth *et al.* 2004; Bischof *et al.* 2007). Many *GAL4* transgenes, most notably the GMR-GAL4 collection from the Janelia Research Campus, have been inserted at the *attP2* locus (Jenett *et al.* 2012). To directly investigate gene

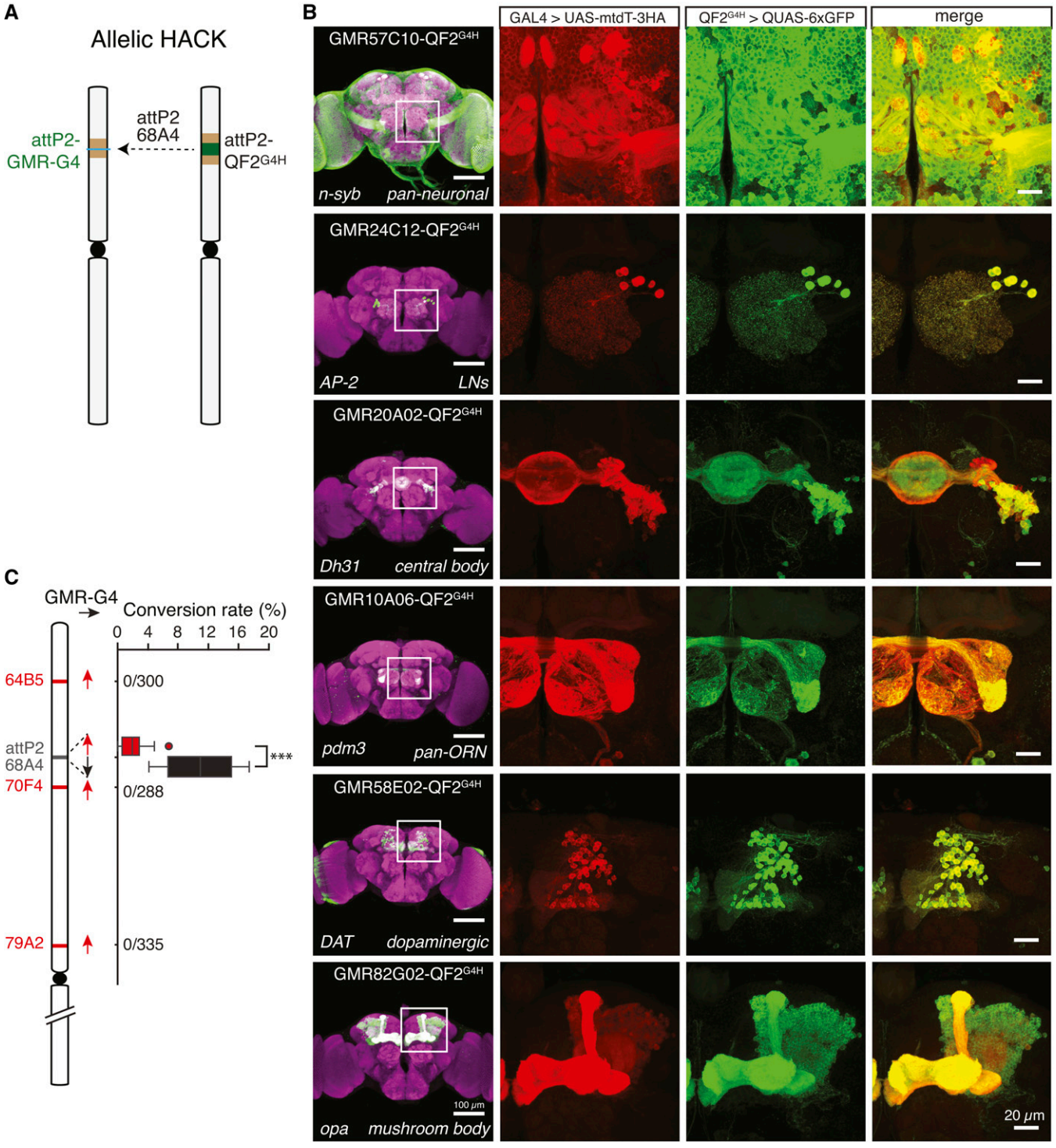

Figure 6 Donor and target inserted at the same loci do not necessarily lead to high conversion frequencies. (A) An *attB-QF2^{G4H}* donor insert at the *attP2* site is used to HACK Janelia *GMR-GAL4* lines inserted at *attP2*. (B) Examples of *QF2* lines that were HACKed from widely used *attP2-GMR-GAL4* lines. Colabeling experiments demonstrate expression patterns of *QF2^{G4H}* recapitulate those of the original *attP2-GMR-GAL4* insertion. Bar, 100 μm (brains, left panel), 20 μm (inset magnification). (C) The conversion rate of *attP2-GMR-GAL4* lines using *attP2-QF2^{G4H}* or nearby *QF2^{G4H}* lines. The *attP2-QF2^{G4H}* donors were either in forward (black arrow, as generated by *pBPGUw-HACK_G4 > QF2*) or reverse (red arrow, as generated by *pHACK_G4 > QF2*) orientations. Both exhibited significantly higher success rates than three nearby donors (ANOVA, $P < 0.001$). The conversion rate mediated by *attP2-QF2^{G4H}* in the same orientation as *attP2-GMR-GAL4* was significantly higher than the conversion rate mediated by *attP2-QF2^{G4H}* inserted in the opposite orientation ($P = 4.7 \times 10^{-5}$, Student's *t*-test).

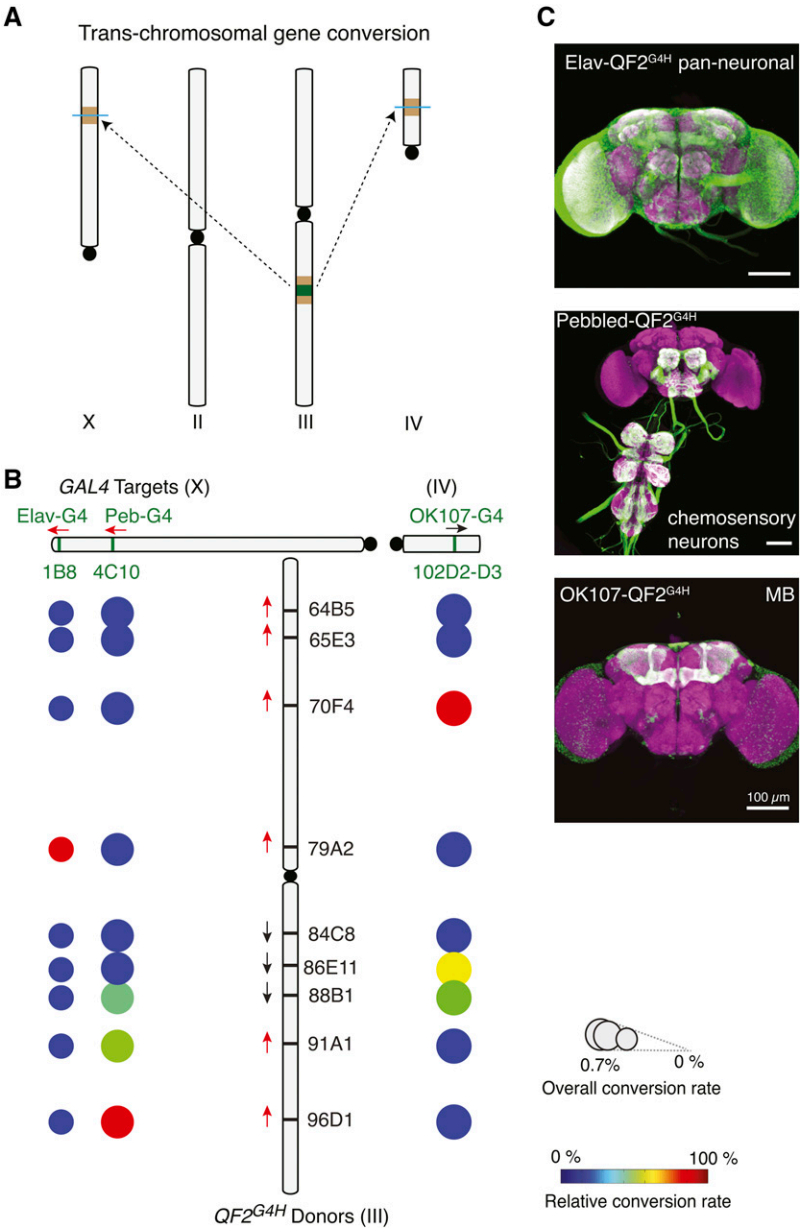

Figure 7 HACK can be used for *trans*-chromosomal gene conversion. (A) Schematic demonstrating the use of a third chromosome $QF2^{G4H}$ donor to HACK target *GAL4* lines on the *X* (*Elav-GAL4*, *pebbled-GAL4*) and fourth chromosomes (*OK107-GAL4*). (B) Results summarizing the efficiency of *trans*-chromosomal HACKing using different donor lines on the third chromosome. See Figure 4 legend for explanation of schematics. (C) The expression patterns of converted $QF2^{G4H}$ lines are consistent with the original *GAL4* lines. Bar, 100 μm.

conversion from the same genomic locus, we inserted $QF2^{G4H}$ donor constructs at the *attP2* locus (Figure 6A). The donor lines would be of special interest to the *Drosophila* community since >7000 GMR *GAL4* lines have been targeted to the *attP2* site.

With the *attP2-*$QF2^{G4H}$ donors, eight commonly-ordered *attP2-GMR-GAL4* lines were successfully converted to $QF2^{G4H}$ and expression patterns were consistent with those of the original GAL4 as shown in the colabeling experiments (Figure 6B, Figure S9, and Table 2). Interestingly, HACK efficiency differed if *attP2-*$QF2^{G4H}$ was inserted in the same or opposite orientation relative to *attP2-GMR-GAL4* (Figure 6C). The efficiency of conversion was low when using the oppositely-oriented *attP2-*$QF2^{G4H}$ donor (Figure 6C red box plot, 2.02 ± 0.5 (SEM) %, $n = 15$ F_1 crosses with a total of 3,014 F_2 males). The HACK efficiency was five times higher when using the *attP2-*$QF2^{G4H}$ donor in the same orientation as the *GMR-GAL4* lines (Figure 6C black box plot, 10.9 ± 2.8 (SEM) %, $n = 4$ F_1 crosses with a total of 943 F_2 males). This confirms the results described for other genomic locations that the relative orientation of donor and target influence conversion efficiency (Figure 5A).

Donor and targets inserted at allelic sites should represent maximal conversion efficiencies. However, the observed allelic conversion rate of ~10% was low relative to other genomic locations (*e.g.*, *OK371* demonstrates ~60% conversion efficiency). To understand if a low conversion rate was due to the attP2 $QF2^{G4H}$ donor, we tested three other $QF2^{G4H}$ donors inserted in genomic locations close to *attP2* (64B5, 70F4, and 79A2) paired with three different GMR lines (*GMR57C10-GAL4*, *GMR20A02-GAL4*, and *GMR24C12-GAL4*). None of them were successful in generating a $QF2^{G4H}$ line ($n = 9$ F_1

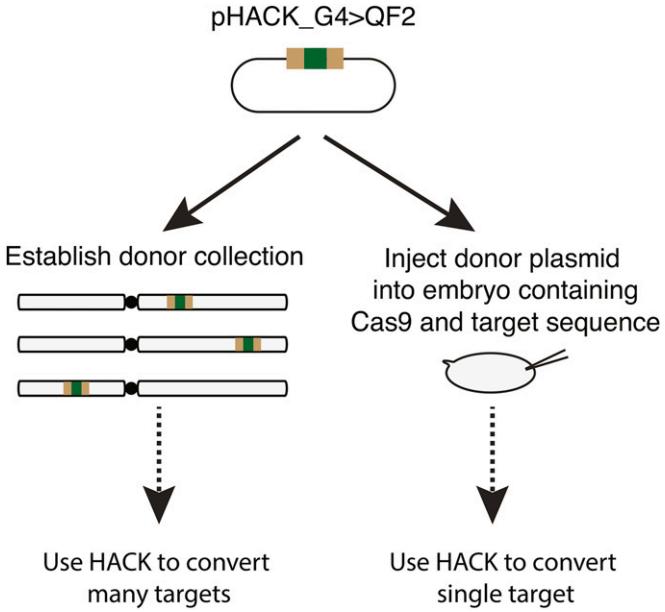

Figure 8 The HACK method can be used with embryo injections to convert a single target at a time. The HACK donor plasmid can be used to generate a collection of integrated donors for use in converting many targets via genetic crosses. Alternatively, the HACK donor plasmid can be injected directly into embryos containing a target and a source of germline Cas9. See Figure S10 for details.

crosses with a total of 1,769 F_2 males) (Figure 6C). The HACK method can be divided into two sequential steps: CRISPR/Cas9 generates a DSB in a target locus, followed by HDR-mediated insertion of exogenous donor DNA. To determine if *GAL4* sequences had been successfully targeted by CRISPR/Cas9, we genotyped individual GAL4$^+$ F_2 males from the F_1 HACK cross that had not been successfully converted (Figure 2B, *GAL4* w^+ positive but *QF2^{G4H} 3xP3-RFP* negative). All examined F_2 males with only the w^+ marker showed indel mutations at the gRNA targeted sequences (N = 10; Figure S7). These results suggest that DSBs at the *attP2* locus occur efficiently, but HDR is limited. Thus the *attP2* locus might be a cold spot for HDR.

HACK can mediate trans-chromosomal gene conversion

We next asked if the HACK strategy could be applied to targets and donors on different chromosomes. When HDR is used for DSB repair, damaged ends search the whole genome for homologous sequences (Szostak *et al.* 1983). Thus, *trans*-chromosomal HACK might work, but it would be expected to be less efficient. Indeed, pan-neuronal (*elav-GAL4*) and pan-chemosensory (*pebbled-GAL4*) target *GAL4* lines on the *X* chromosome were successfully HACKed by *QF2^{G4H}* donors on the third chromosome (Figure 7). This *trans*-chromosomal HACK strategy was not limited to targets on the *X* chromosome. The pan-mushroom body *GAL4* line, *OK107-GAL4*, on the fourth chromosome could be HACKed by *QF2^{G4H}* donors on the third chromosome (Figure 7 and Figure S8). The overall conversion rate in *trans*-chromosomal HACK was low, as expected (0.3–0.7%). We reasoned that this was the result of inefficient HDR and sequenced non-HACKed F_2 *GAL4* flies (*GAL4* w^+ positive but *QF2^{G4H} 3xP3-RFP* negative). Indeed, all GAL4+ flies examined revealed indel mutations, indicating successful DSB events at the *GAL4* sequence (N = 6, Figure S8B). In summary, these results suggest that *trans*-chromosomal HACKing is possible, albeit at a reduced frequency.

The HACK method is applicable to direct embryo injection of a pHACK donor plasmid

In cases in which only a single HACK target conversion is required, it might be preferable to directly inject a HACK donor plasmid into a target strain instead of first generating a donor HACK collection (Figure 8). We thus tested if the *pHACK_G4 > QF2* plasmid DNA could be used directly as a donor for HACK-mediated conversion when injected into embryos containing Cas9 endonuclease (Gratz *et al.* 2014) and *GAL4* target sequence. Using *Vas-Cas9*; *OK371-GAL4* as the injection strain, we successfully converted *OK371-GAL4* into *OK371-QF2^{G4H}* using standard embryo injection procedures with a success rate of 5.8% (64/1107 G_1 males) (Figure S10).

Discussion

We developed a genetic method that uses endogenous HDR mechanisms to modify existing transgenic components. The HACK method allows *GAL4* lines to be converted to *QF2* lines via two sequential crosses. The genetic crosses combine CRISPR/Cas9-mediated gene conversion with a transgenic donor cassette to introduce *T2A-QF2* elements into a *GAL4* target. This allows QF2 protein to be expressed instead of a functional GAL4. The HACK technique is easy and efficient, and can be adapted to introduce other donor sequences. Instead of conducting multiple laborious, expensive, and time-consuming injections and screens aimed at introducing and characterizing different genetic elements, the HACK technique could be applied to convert essentially any *GAL4* line into a range of different genetic reagents, such as *GAL80*, *split-GAL4*, *LexA*, *FLPase*, *Cre*, *attP*, *FRT*, and more. Future HACK donors could also be designed to replace the entire *GAL4* gene by targeting 5′ and 3′ homologous components specific to the target transgenic sequence (*e.g.*, the 5′ *DSCP* promoter and 3′ yeast terminator sequences in *GMR-GAL4* insertions). Similarly, the HACK technique could be applied to other transgenic sequences besides *GAL4* for conversion. This simplifies strategies aimed at generating transgenes containing different genetic components.

The recommended approach to HACK a *GAL4* line to a *QF2* line involves two steps. The first is to map the target *GAL4* line for conversion (Potter and Luo 2010) (if its position is not already known). The second is to proceed with crosses outlined in Figure 2 with 2–3 *QF2^{G4H}* donor lines that map closest to the target *GAL4* region. Conversion efficiencies will depend on the orientation of the *GAL4* target and *QF2^{G4H}* donors, but a successful conversion typically required screening ~150 w^+ F_2 progeny. If the *GAL4* target is in a cold spot, then more F_2 progeny may need to be screened. All 24 HACK

conversion phenotypes we detected (showing both w^+ and *RFP+)* represented actual conversion events, and we did not detect any false positives. This suggests that screening could be terminated after finding a single positive conversion phenotype.

P-element swapping is a previously developed unique genetic strategy for changing existing *P*-element transgenic lines (Sepp and Auld 1999). This technique relies on targeted transposition, in which one *P* element acts as a homology source for an excised *P* element that has left behind small homology arms (Sepp and Auld 1999). The efficiency of *P*-element swapping is low: at best, ~1.5% of all single F_1 male crosses will yield any *P*-element-swapped progeny (Sepp and Auld 1999). In comparison, the HACK method at best requires only a single F_1 cross to yield a swap (*e.g.*, 100% efficiency). In addition, the crossing schemes required for *P*-element swapping are more complicated, and since it requires the replacement of one *P* element for another, it cannot be applied to transgenic components generated using other transposons, such as piggyBac (Handler *et al.* 1998) or Minos (Metaxakis *et al.* 2005). Furthermore, since piggyBac and Minos elements excise precisely during transposition, transgenes generated by these elements are not amendable to similar transposase-mediated replacement strategies.

The QF2-driven expression patterns were similar to the GAL4 expression patterns and levels for most converted lines. However, there were exceptions. For example, *GH146-QF2^{G4H}* generally drove weaker reporter expression than the original *GH146-GAL4*. In addition, some *GMR-GAL4* lines, such as *GMR10A06-GAL4*, *GMR71G10-GAL4*, and *GMR16A06-GAL4*, exhibited very weak *QUAS* reporter expression after conversion to *T2A-QF2* lines (Figure S9). Interestingly, *QF2* transgenes generated based on these same GMR enhancer sequences were also very weak (O. Schuldiner, personal communication), suggesting that the problem is not with the activity of the *T2A-QF2*. Instead, it suggests that the intrinsic properties of the *GAL4* or *QF2* DNA sequences may influence expression of the targeted line.

Characterization of the HACK technique required investigation into the efficiencies of using different target and donor pairs for HDR. As such, it represents an *in vivo* system for investigating allelic/ectopic gene conversion in a model genetic animal. Gene conversion has been examined at a limited set of target genes and homologous donor loci. Due to intergene differences, the data sets could not be compared (Chen *et al.* 2007). The HACK system provides the first opportunity to comprehensively investigate how genomic location affects gene conversion across the genome. We identified target *GAL4* sites that exhibited greatly increased (hot) or greatly decreased (cold) rates of HACK conversion. Of the 25 GAL4 lines we attempted to HACK, only 1 GAL4 target proved unable to convert in two attempts: *en2.4-GAL4* (in crosses to the seven *QF2^{G4H}* HACK donor lines on the second chromosome). Since ubiquitous or pan-tissue GAL4 lines can be converted, failure to convert was unlikely due to acquired expression of QF2. Instead, it is possible that *en2.4-GAL4* represents an extreme cold spot. The reason for the observed variation in HACK efficiencies is unknown. One possible explanation is that local genomic structure could prevent Cas9-mediated excision at the DNA (Horlbeck *et al.* 2016). However, our data suggest this is unlikely. We found that cold spots (such as the *OK107-GAL4* insertion site and *attP2-GAL4*) were efficiently targeted for DSB by CRISPR/Cas9. Instead, it suggests that HDR mechanisms are not equally efficient throughout the genome, and cold spots represent loci with repressed HDR activity. A previous study in yeast suggested a correlation between local transcription and HDR efficiency of the target, but the precise mechanism underlying this correlation remains unknown (Gonzalez-Barrera *et al.* 2002). A recent technique called mutagenic chain reaction (MCR) uses HDR to generate self-copying mutations in a target gene at high frequency (Gantz and Bier 2015). Our work suggests that MCR may not be equally applicable to all genomic loci.

The HACK technique also indicates that single integrated compatible donor sequences at distant locations can be used for HDR. For example, we were able to generate gene conversions to the *X* and fourth chromosomes using a donor sequence on the third chromosome. This suggests that techniques like MCR could be jump-started by a random integration of a compatible MCR transgene, which might prove to be easier to achieve in nonmodel organisms such as mosquitoes. Similarly, gene conversion using compatible HACK insertions might provide possible strategies for gene therapy in disease tissues (Chen *et al.* 2007) or as a reliable mechanism to introduce targeted genomic knock-ins in insect and mammalian systems.

Acknowledgments

We thank E. Marr for splinkerette genetic mapping of the *GAL4* and *QF2^{G4H}* donor lines in this study. We thank Q. Liu, D. Task, and R. Reed for comments on the manuscript and the Potter laboratory members for discussions. We thank A. Parks at Bloomington *Drosophila* Stock Center for providing a list of the frequently ordered stocks from 01/01/2013 to 10/01/2015. Stocks were obtained from the Bloomington *Drosophila* Stock Center (National Institutes of Health P40OD018537). We thank the Center for Sensory Biology Imaging Facility (National Institutes of Health P30 DC-005211) for LSM710 confocal microscopy. This work was supported by National Institutes of Health grants from the National Institute on Deafness and Other Communication Disorders (R01 DC-013070) and National Institute of Neurological Disorders and Stroke (R21 NS-088521). The authors declare no competing financial interests.

Author contributions: C.-C.L. and C.J.P. conceived and designed the experiments. C.-C.L. performed the experiments. C.-C.L. analyzed the data. C.-C.L. generated the DNA and transgenic reagents and materials. C.-C.L. and C.J.P wrote the paper.

Literature Cited

Bernstein, K. A., and R. Rothstein, 2009 At loose ends: resecting a double-strand break. Cell 137: 807–810.

Bischof, J., R. K. Maeda, M. Hediger, F. Karch, and K. Basler, 2007 An optimized transgenesis system for Drosophila using germ-line-specific phiC31 integrases. Proc. Natl. Acad. Sci. USA 104: 3312–3317.

Brand, A. H., and N. Perrimon, 1993 Targeted gene expression as a means of altering cell fates and generating dominant phenotypes. Development 118: 401–415.

Chen, J.-M., D. N. Cooper, N. Chuzhanova, C. Férec, and G. P. Patrinos, 2007 Gene conversion: mechanisms, evolution and human disease. Nat. Rev. Genet. 8: 762–775.

Cong, L., F. A. Ran, D. Cox, S. Lin, R. Barretto *et al.*, 2013 Multiplex genome engineering using CRISPR/Cas systems. Science 339: 819–823.

Diao, F., and B. H. White, 2012 A novel approach for directing transgene expression in Drosophila: T2A-Gal4 in-frame fusion. Genetics 190: 1139–1144.

Diao, F., H. Ironfield, H. Luan, F. Diao, W. C. Shropshire *et al.*, 2015 Plug-and-Play Genetic Access to Drosophila Cell Types using Exchangeable Exon Cassettes. Cell Reports 10: 1410–1423.

Doudna, J. A., and E. J. Sontheimer, 2014 *The Use of CRISPR/cas9, ZFNs, TALENs in Generating Site Specific Genome Alterations* (Methods in Enzymology, Vol. 546). Academic Press, San Diego.

Engels, W. R., D. M. Johnson-Schlitz, W. B. Eggleston, and J. Sved, 1990 High-frequency P element loss in Drosophila is homolog dependent. Cell 62: 515–525.

Engels, W. R., C. R. Preston, and D. M. Johnson-Schlitz, 1994 Long-range cis preference in DNA homology search over the length of a Drosophila chromosome. Science 263: 1623–1625.

Gandhi, M., V. N. Evdokimova, K. T. Cuenco, M. N. Nikiforova, L. M. Kelly *et al.*, 2012 Homologous chromosomes make contact at the sites of double-strand breaks in genes in somatic G0/G1-phase human cells. Proc. Natl. Acad. Sci. USA 109: 9454–9459.

Gantz, V. M., and E. Bier, 2015 The mutagenic chain reaction: A method for converting heterozygous to homozygous mutations. Science 348: 442–444.

Gloor, G. B., N. A. Nassif, D. M. Johnson-Schlitz, C. R. Preston, and W. R. Engels, 1991 Targeted gene replacement in Drosophila via P element-induced gap repair. Science 253: 1110–1117.

Gnerer, J. P., K. J. T. Venken, and H. A. Dierick, 2015 Gene-specific cell labeling using MiMIC transposons. Nucleic Acids Res. 43: e56.

Gohl, D. M., M. A. Silies, X. J. Gao, S. Bhalerao, F. J. Luongo *et al.*, 2011 A versatile in vivo system for directed dissection of gene expression patterns. Nat. Methods 8: 231–237.

Gonzalez-Barrera, S., M. Garcia-Rubio, and A. Aguilera, 2002 Transcription and double-strand breaks induce similar mitotic recombination events in Saccharomyces cerevisiae. Genetics 162: 603–614.

Gratz, S. J., A. M. Cummings, J. N. Nguyen, D. C. Hamm, L. K. Donohue *et al.*, 2013 Genome engineering of Drosophila with the CRISPR RNA-guided Cas9 nuclease. Genetics 194: 1029–1035.

Gratz, S. J., F. P. Ukken, C. D. Rubinstein, G. Thiede, L. K. Donohue *et al.*, 2014 Highly Specific and Efficient CRISPR/Cas9-Catalyzed Homology-Directed Repair in Drosophila. Genetics 196: 961–971.

Groth, A. C., M. Fish, R. Nusse, and M. P. Calos, 2004 Construction of transgenic Drosophila by using the site-specific integrase from phage phiC31. Genetics 166: 1775–1782.

Hadjieconomou, D., S. Rotkopf, C. Alexandre, D. M. Bell, B. J. Dickson *et al.*, 2011 Flybow: genetic multicolor cell labeling for neural circuit analysis in Drosophila melanogaster. Nat. Methods 8: 260–266.

Handler, A. M., S. D. McCombs, M. J. Fraser, and S. H. Saul, 1998 The lepidopteran transposon vector, piggyBac, mediates germ-line transformation in the Mediterranean fruit fly. Proc. Natl. Acad. Sci. USA 95: 7520–7525.

Horlbeck, M. A., L. B. Witkowsky, B. Guglielmi, J. M. Replogle, L. A. Gilbert *et al.*, 2016 Nucleosomes impede Cas9 access to DNA in vivo and in vitro. eLife 5: e12677.

Hsu, P. D., D. A. Scott, J. A. Weinstein, F. A. Ran, S. Konermann *et al.*, 2013 DNA targeting specificity of RNA-guided Cas9 nucleases. Nat. Biotechnol. 31: 827–832.

Ito, K., W. Awano, K. Suzuki, Y. Hiromi, and D. Yamamoto, 1997 The Drosophila mushroom body is a quadruple structure of clonal units each of which contains a virtually identical set of neurones and glial cells. Development 124: 761–771.

Jefferis, G. S. X. E., C. J. Potter, A. M. Chan, E. C. Marin, T. Rohlfing *et al.*, 2007 Comprehensive maps of Drosophila higher olfactory centers: spatially segregated fruit and pheromone representation. Cell 128: 1187–1203.

Jenett, A., G. M. Rubin, T.-T. B. Ngo, D. Shepherd, C. Murphy *et al.*, 2012 A GAL4-Driver Line Resource for Drosophila Neurobiology. Cell Reports 2: 991–1001.

Jinek, M., K. Chylinski, I. Fonfara, M. Hauer, J. A. Doudna *et al.*, 2012 A programmable dual-RNA-guided DNA endonuclease in adaptive bacterial immunity. Science 337: 816–821.

Komiyama, T., J. R. Carlson, and L. Luo, 2004 Olfactory receptor neuron axon targeting: intrinsic transcriptional control and hierarchical interactions. Nat. Neurosci. 7: 819–825.

Lai, S.-L., and T. Lee, 2006 Genetic mosaic with dual binary transcriptional systems in Drosophila. Nat. Neurosci. 9: 703–709.

Lee, C.-S., R. W. Wang, H.-H. Chang, D. Capurso, M. R. Segal *et al.*, 2016 Chromosome position determines the success of double-strand break repair. Proc. Natl. Acad. Sci. USA 113: E146–E154.

Levis, R., T. Hazelrigg, and G. M. Rubin, 1985 Effects of genomic position on the expression of transduced copies of the white gene of Drosophila. Science 229: 558–561.

Lieber, M. R., 2010 The mechanism of double-strand DNA break repair by the nonhomologous DNA end-joining pathway. Annu. Rev. Biochem. 79: 181–211.

Metaxakis, A., S. Oehler, A. Klinakis, and C. Savakis, 2005 Minos as a genetic and genomic tool in Drosophila melanogaster. Genetics 171: 571–581.

Pfeiffer, B. D., A. Jenett, A. S. Hammonds, T.-T. B. Ngo, S. Misra *et al.*, 2008 Tools for neuroanatomy and neurogenetics in Drosophila. Proc. Natl. Acad. Sci. USA 105: 9715–9720.

Port, F., H. M. Chen, T. Lee, and S. L. Bullock, 2014 Optimized CRISPR/Cas tools for efficient germline and somatic genome engineering in Drosophila. Proc. Natl. Acad. Sci. USA 111: E2967–E2976.

Potter, C. J., and L. Luo, 2010 Splinkerette PCR for mapping transposable elements in Drosophila. PLoS One 5: e10168.

Potter, C. J., B. Tasic, E. V. Russler, L. Liang, and L. Luo, 2010 The Q system: a repressible binary system for transgene expression, lineage tracing, and mosaic analysis. Cell 141: 536–548.

Ren, X., J. Sun, B. E. Housden, Y. Hu, C. Roesel *et al.*, 2013 Optimized gene editing technology for Drosophila melanogaster using germ line-specific Cas9. Proc. Natl. Acad. Sci. USA 110: 19012–19017.

Riabinina, O., D. Luginbuhl, E. Marr, S. Liu, M. N. Wu *et al.*, 2015 Improved and expanded Q-system reagents for genetic manipulations. Nat. Methods 12: 219–222.

Rong, Y. S., and K. G. Golic, 2000 Gene targeting by homologous recombination in Drosophila. Science 288: 2013–2018.

Sepp, K. J., and V. J. Auld, 1999 Conversion of lacZ enhancer trap lines to GAL4 lines using targeted transposition in Drosophila melanogaster. Genetics 151: 1093–1101.

Shearin, H. K., I. S. Macdonald, L. P. Spector and R. S. Stowers, 2014 Hexameric GFP and mCherry Reporters for the Drosophila GAL4, Q, and LexA Transcription Systems. Genetics. 196: 951–960.

Siegal, M. L., and D. L. Hartl, 1996 Transgene Coplacement and high efficiency site-specific recombination with the Cre/loxP system in Drosophila. Genetics 144: 715–726.

Sweeney, L. B., A. Couto, Y.-H. Chou, D. Berdnik, B. J. Dickson *et al.*, 2007 Temporal target restriction of olfactory receptor neurons by Semaphorin-1a/PlexinA-mediated axon-axon interactions. Neuron 53: 185–200.

Szostak, J. W., T. L. Orr-Weaver, R. J. Rothstein, and F. W. Stahl, 1983 The double-strand-break repair model for recombination. Cell 33: 25–35.

Venken, K. J. T., K. L. Schulze, N. A. Haelterman, H. Pan, Y. He *et al.*, 2011 MiMIC: a highly versatile transposon insertion resource for engineering Drosophila melanogaster genes. Nat. Methods 8: 737–743.

Yoshihara, M., and K. Ito, 2000 Improved Gal4 screening kit for large-scale generation of enhancer-trap strains. Drosoph. Inf. Serv. 83: 199–202.

Communicating editor: N. Perrimon

GENETICS

Supporting Information
www.genetics.org/lookup/suppl/doi:10.1534/genetics.116.191783/-/DC1

Editing Transgenic DNA Components by Inducible Gene Replacement in *Drosophila melanogaster*

Chun-Chieh Lin and Christopher J. Potter

DOI: 10.1534/genetics.116.191783

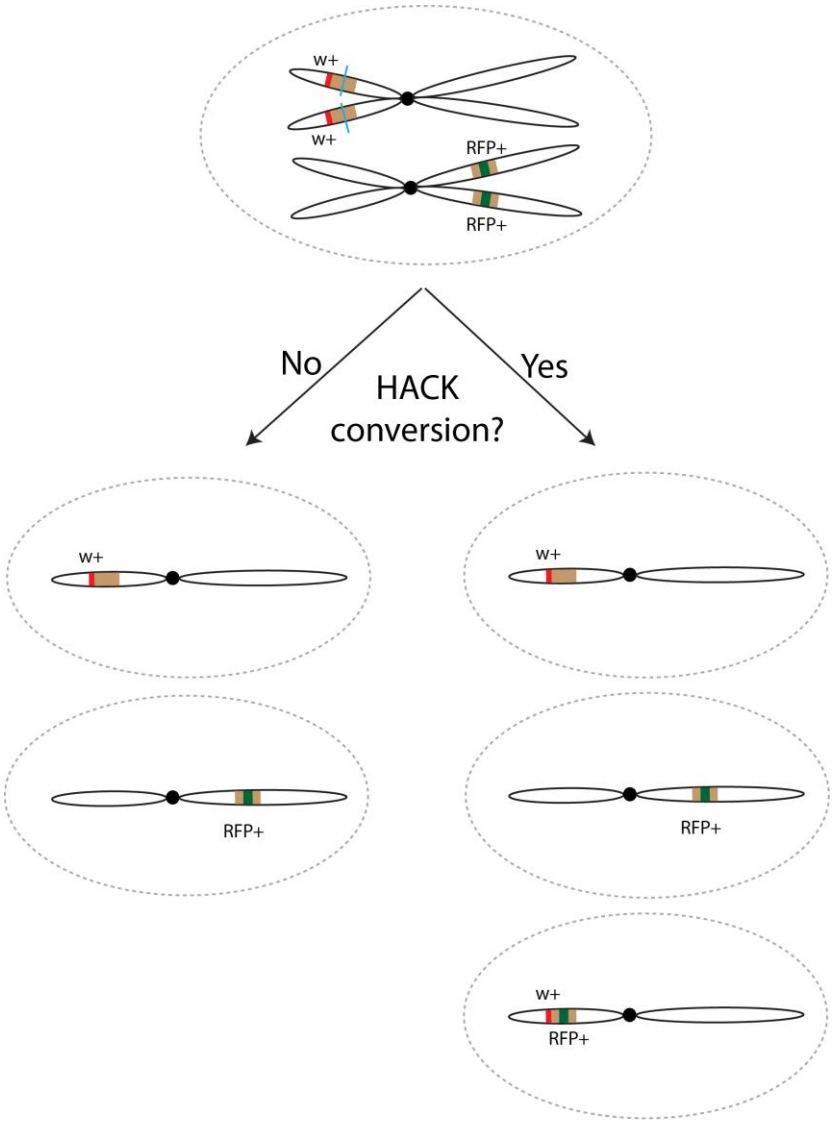

$$\text{Conversion rate} = \frac{(\text{No. of } w^{+}\ RFP+ \text{ flies})}{(\text{No. of } w^{+}\ RFP- \text{ flies}) + (\text{No. of } w^{+}\ RFP+ \text{ flies})}$$

Figure S1: Schematic illustration of HACK in the meiotic germline cells. Since *Drosophila* males do not undergo chromosomal recombination during meiosis, the haploid gametes contain either w^{+} or *RFP+* chromosome with a 1:1 ratio (left). A HACK event creates a DSB and inserts donor sequences into the target site. The process incorporates an *RFP+* marker into the transgene that already contains a w^{+} marker. Thus, a successful HACK conversion generates gametes with double markers (right). The conversion rate is defined as the number of progeny with double markers (w^{+} *RFP+*) divided by all progenies with the target w^{+} marker (w^{+} *RFP-* and w^{+} *RFP+).*

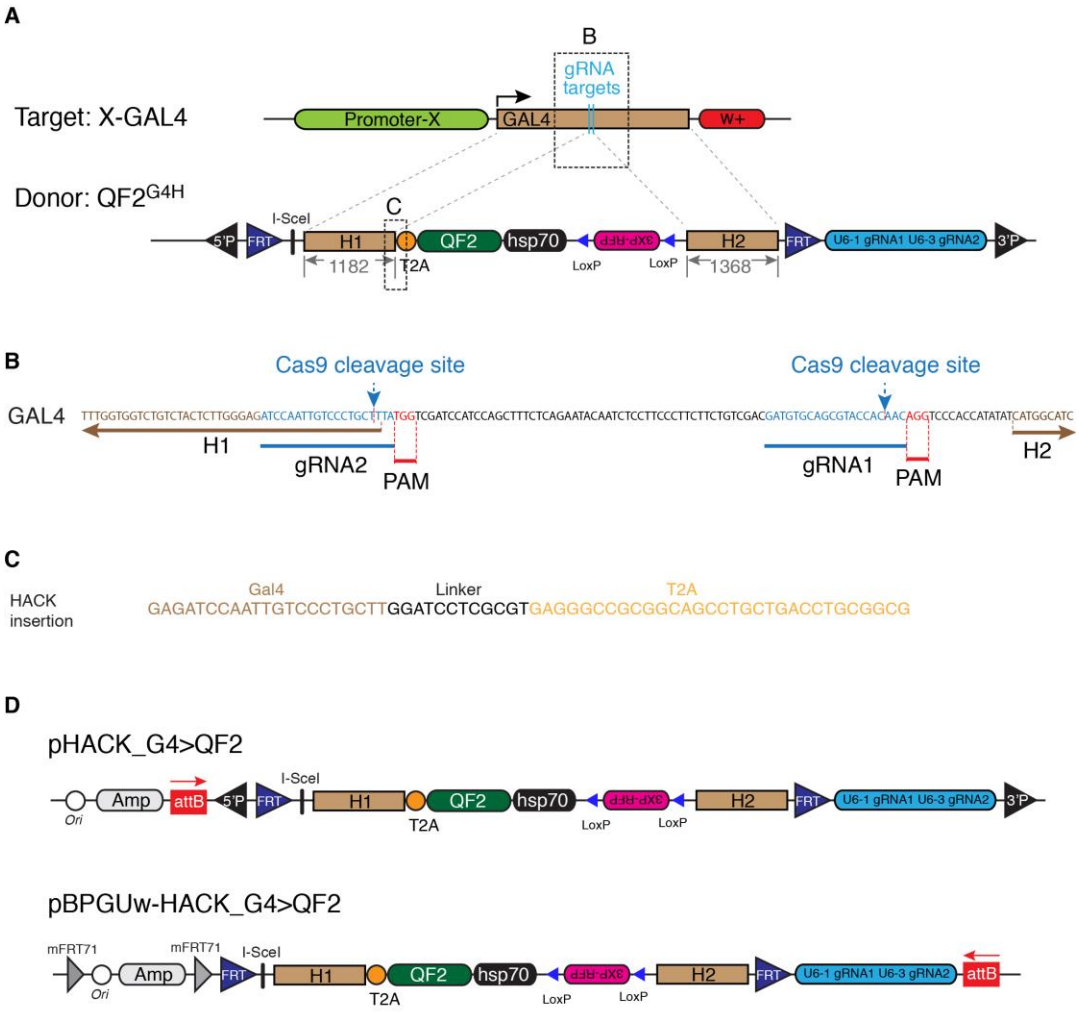

Figure S2: Details for the sites of Cas9 cleavage and homology arms utilized by *QF2^{G4H}* (**A**) Schematic of the *GAL4* target and *QF2^{G4H}* donor. The boxed regions are shown in **B-C**. (**B**) Sequence of *GAL4* highlighting the gRNA target sites and homology arms. The homology arms do not contain the *GAL4* gRNA sequences. (**C**) Sequence of the *GAL4-T2A* region inserted during HACK. The linker sequence maintains the GAL4 coding frame. PAM, protospacer adjacent motif (**D**) Schematic of *pHACK_G4>QF2* and *pBPGUw-HACK_G4>QF2* constructs. *AttB* sites in *pHACK_G4>QF2* and *pBPGUw_HACK_G4>QF2* are in opposite orientations.

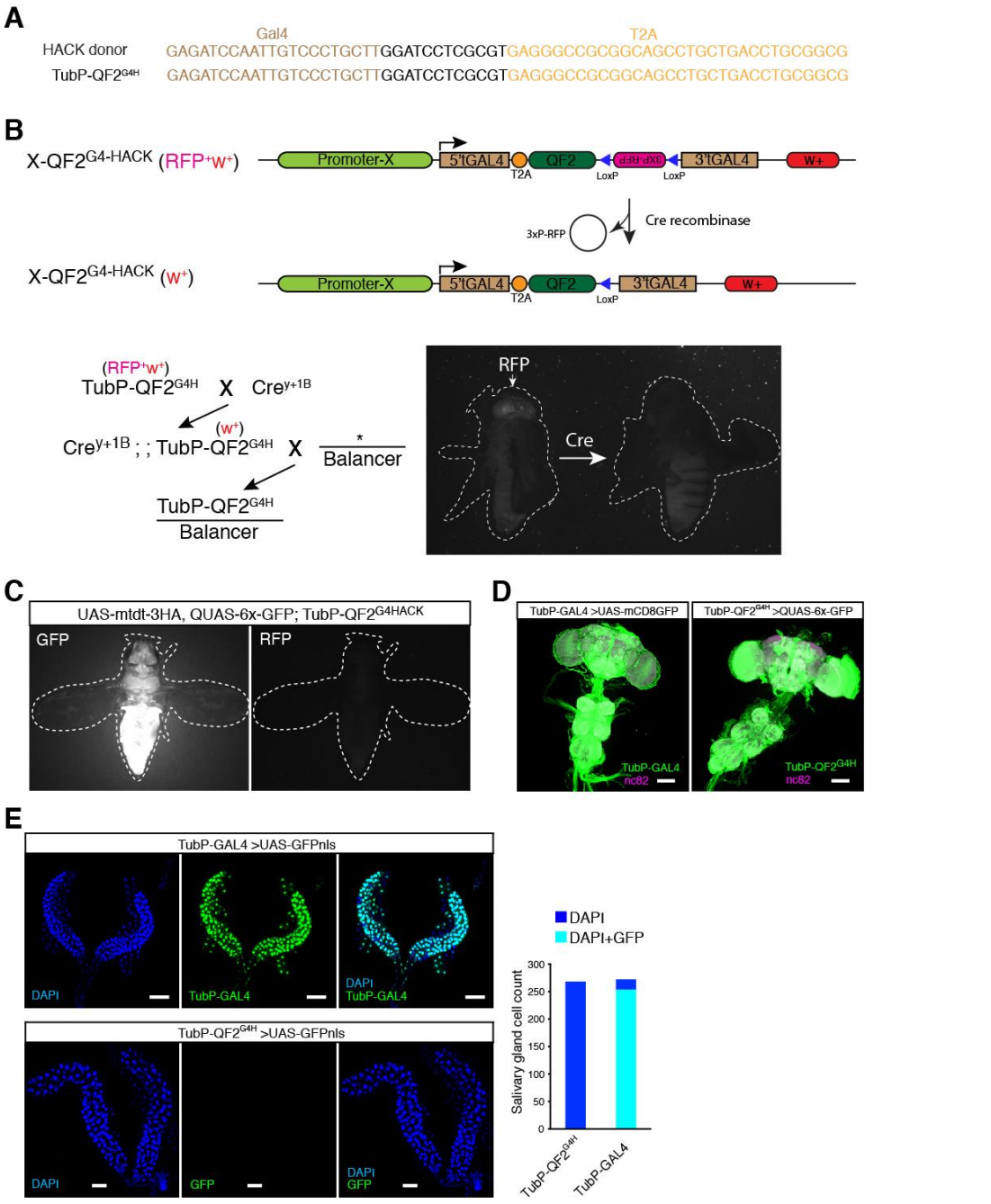

Figure S3: Examining the successful HACK event by using *TubP-QF2^{G4H}* as an example. (**A**) DNA sequencing of *TubP-QF2^{G4H}* confirms successful gene conversion according to the donor sequence. (**B**) Cartoon, crossing scheme, and representative flies illustrating the removal of the *3xP-RFP* marker by Cre recombinase. (**C**) *QF2^{G4H}* specifically drives *QUAS-GFP* reporter expression and does not activate *UAS-mtdT-3HA* reporters. (**D**) Confocal images of adult brains. The *TubP-QF2^{G4H}* expression pattern is consistent with that of *TubP-GAL4*. Scale bar, 100 µm. (**E**) *UAS-GFPnls* reporter expression driven by *TubP-GAL4* or *TubP-QF2^{G4H}* in larval salivary glands. The *TubP-QF2^{G4H}* line exhibited a lack of *GAL4* activity as determined by the absence of GFP signal in the salivary glands (*TubP-QF2^{G4H}>UAS-GFPnls*). Scale bar, 100 µm.

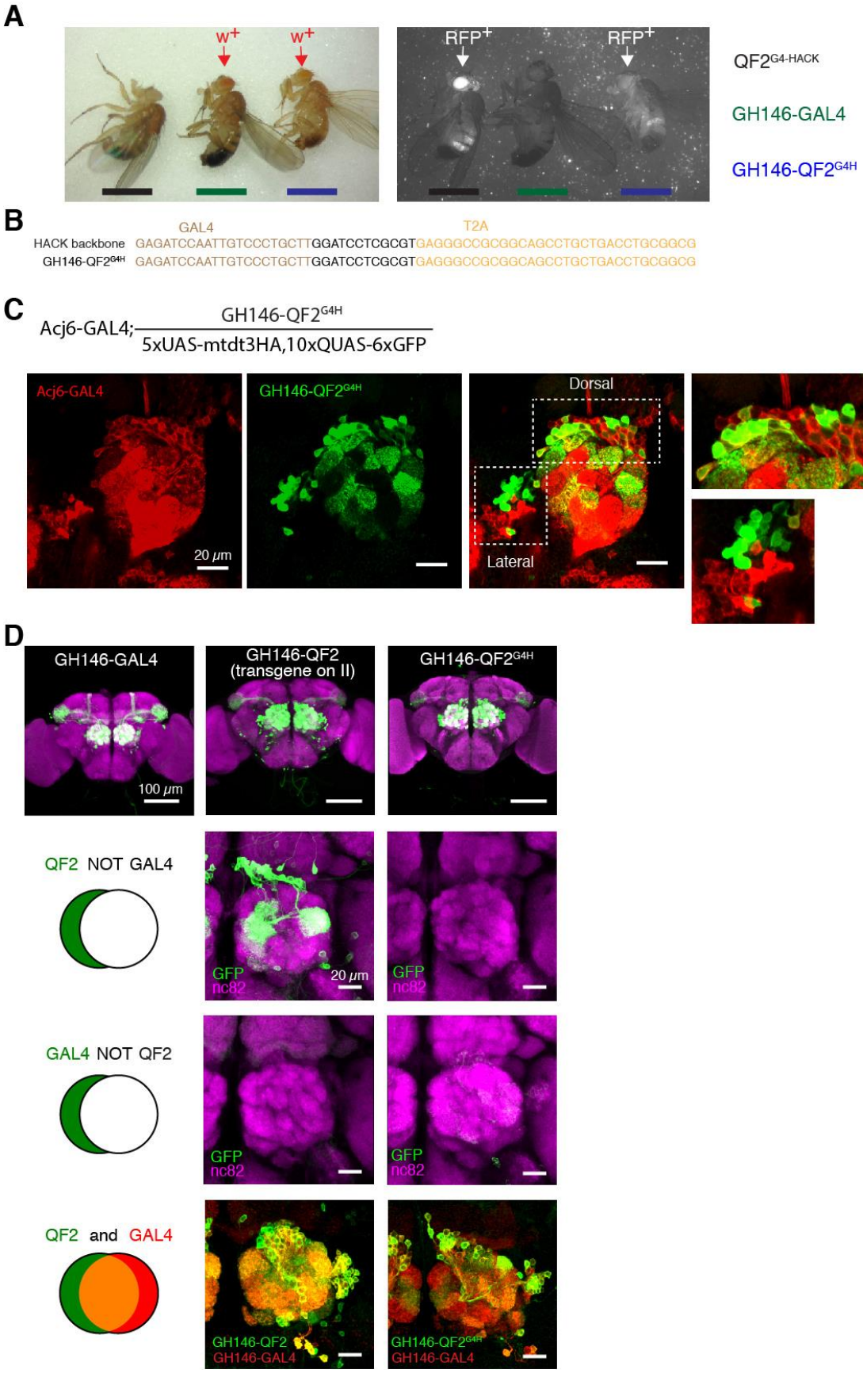
A
w+
w+
RFP+
RFP+
QF2G4-HACK
GH146-GAL4
GH146-QF2G4H
B
GAL4
T2A
HACK backbone GAGATCCAATTGTCCCTGCTTGGATCCTCGCGTGAGGGCCGCGGCAGCCTGCTGACCTGCGGCG
GH146-QF2G4H GAGATCCAATTGTCCCTGCTTGGATCCTCGCGTGAGGGCCGCGGCAGCCTGCTGACCTGCGGCG
C
Acj6-GAL4;GH146-QF2G4H / 5xUAS-mtdt3HA,10xQUAS-6xGFP
Acj6-GAL4
20 μm
GH146-QF2G4H
Dorsal
Lateral
D
GH146-GAL4
100 μm
GH146-QF2 (transgene on II)
GH146-QF2G4H
QF2 NOT GAL4
GFP
nc82
20 μm
GAL4 NOT QF2
QF2 and GAL4
GH146-QF2
GH146-GAL4
GH146-QF2G4H
GH146-GAL4

Figure S4: Intersectional studies using *GH146-QF2^{G4H}* confirm recapitulation of original GAL4 expression. (**A**) Double-positive F_2 males indicate a successful HACK conversion event. (**B**) DNA sequencing results confirm accurate gene conversion. (**C**) *Acj6-GAL4* and *GH146-QF2^{G4H}* partially overlap in a dorsal population of projection neurons. The function of GAL4 driven by the Acj6 promoter in the dorsal projection neurons is not affected by *GH146-QF2^{G4H}*, which expresses a 5' truncated GAL4. (**D**) Transgenic *QF2* lines using the *GH146* promoter do not accurately re-capitulate the original *GH146* enhancer trap line. More neurons are detected in the central part of the brain in transgenic *GH146-QF2* (*GH146-QF2>QUAS-mCD8GFP*). Intersectional studies (QF2 not GAL4) were used to determine similarities of expression patterns. The *GH146-QF2* not *GH146-GAL4* intersection (*GH146-GAL4>UAS-QS, GH146-QF2>QUAS-mCD8GFP*) highlights projection neurons labeled by *GH146-QF2* but not *GH146-GAL4*. The *GH146-QF2^{G4H}* not *GH146-GAL4* intersection (*GH146-GAL4>UAS-QS, GH146-QF2^{G4H}>QUAS-mCD8GFP)* highlights that *GH146-QF2^{G4H}* expression matches (or is a subset) of the *GH146-GAL4* expression pattern. The *GH146-GAL4* not *GH146-QF2* and *GH146-GAL4* not *GH146-QF2^{G4H}* intersectional studies (GAL4 not QF2, *GH146-GAL4>UAS-mCD8GFP, GH146-QF2>QUAS-Gal80 and GH146-GAL4>UAS-mCD8GFP, GH146-QF2^{G4H}>QUAS-Gal80)* highlight that both *GH146-QF2* and *GH146-QF2^{G4H}* express in all projection neurons labeled by *GH146-GAL4*. QF2 and GAL4 intersectional studies demonstrate the overlap in expression patterns (*GH146-QF2>QUAS-mtdT-3HA, GH146-GAL4>UAS-mCD8GFP and GH146-QF2^{G4H}>QUAS-mtdT-3HA, GH146-GAL4>UAS-mCD8GFP*). Scale bars: 100µm (low magnification), 20 µm (antennal lobes).

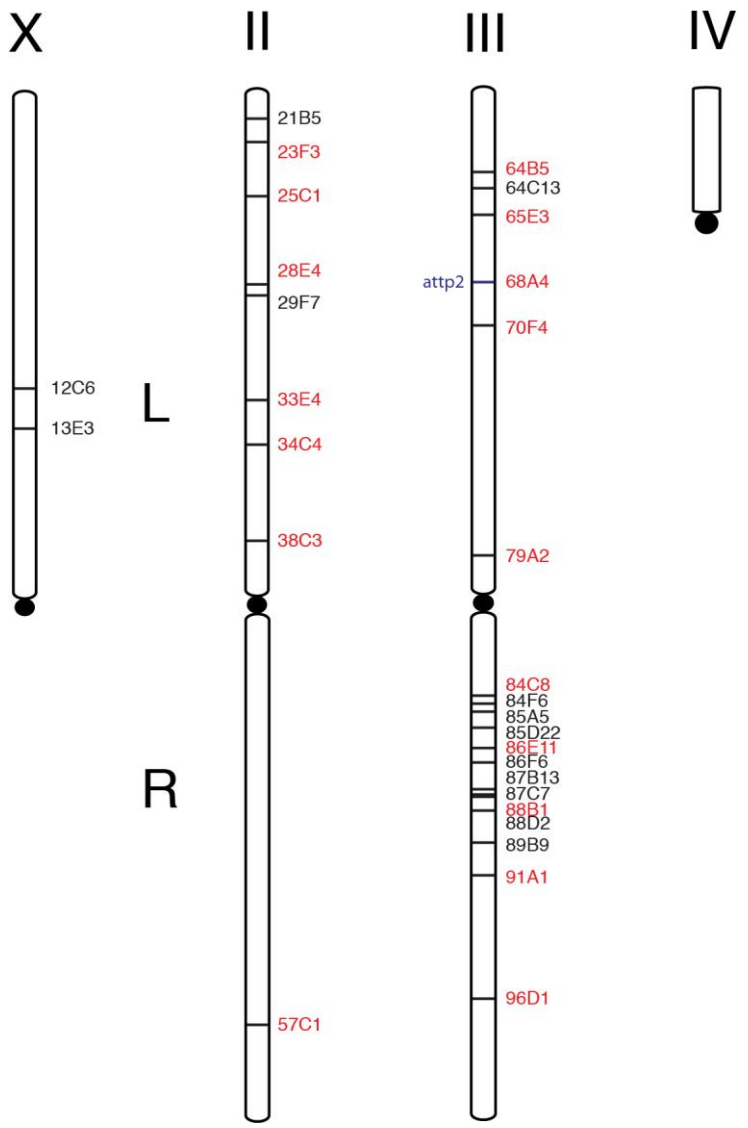

Figure S5: Schematic summary of the *QF2^{G4H}* donor collection. The cytological positions of the P-element transgenes are shown. The insertions used in this study are highlighted in red.

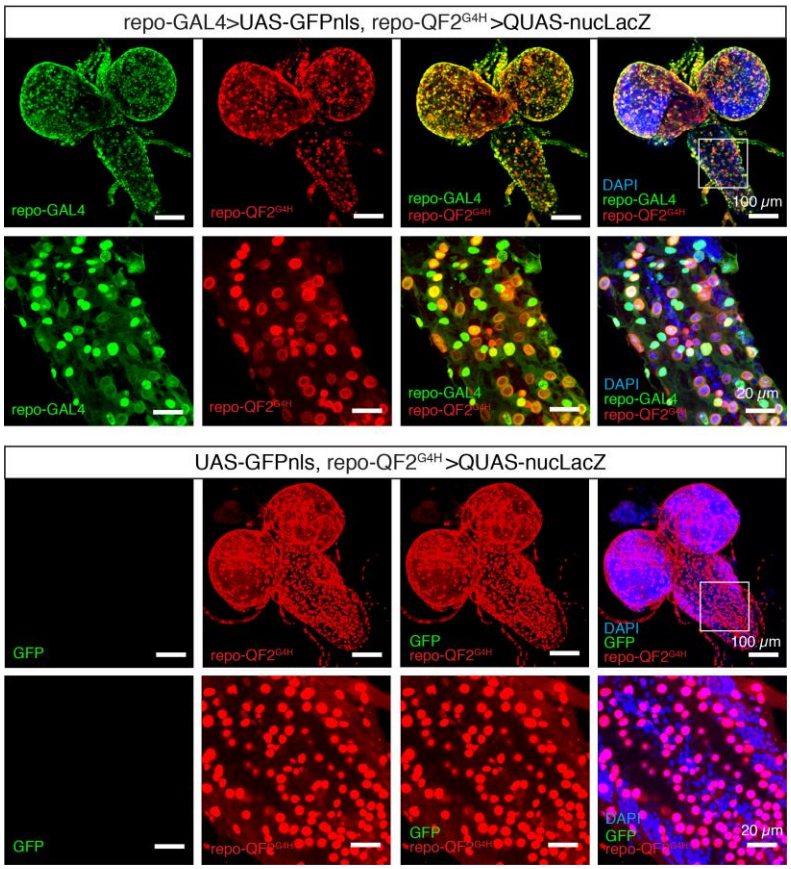

Figure S6: *Repo-QF2^{G4H}* recapitulates the expression pattern of *repo-Gal4*. (Top) Expression of *repo-GAL4* and *repo-QF2^{G4H}* in 2nd instar larvae demonstrates consistent co-labeling. Note that the reporters differentially label the nucleus. (**Bottom**) *Repo-QF2^{G4H}* does not drive expression of a *UAS-GFPnls* reporter. Confocal settings were maintained between the top and bottom set of images. Scale bar: 100 µm (upper panels), 20 µm (lower panels).

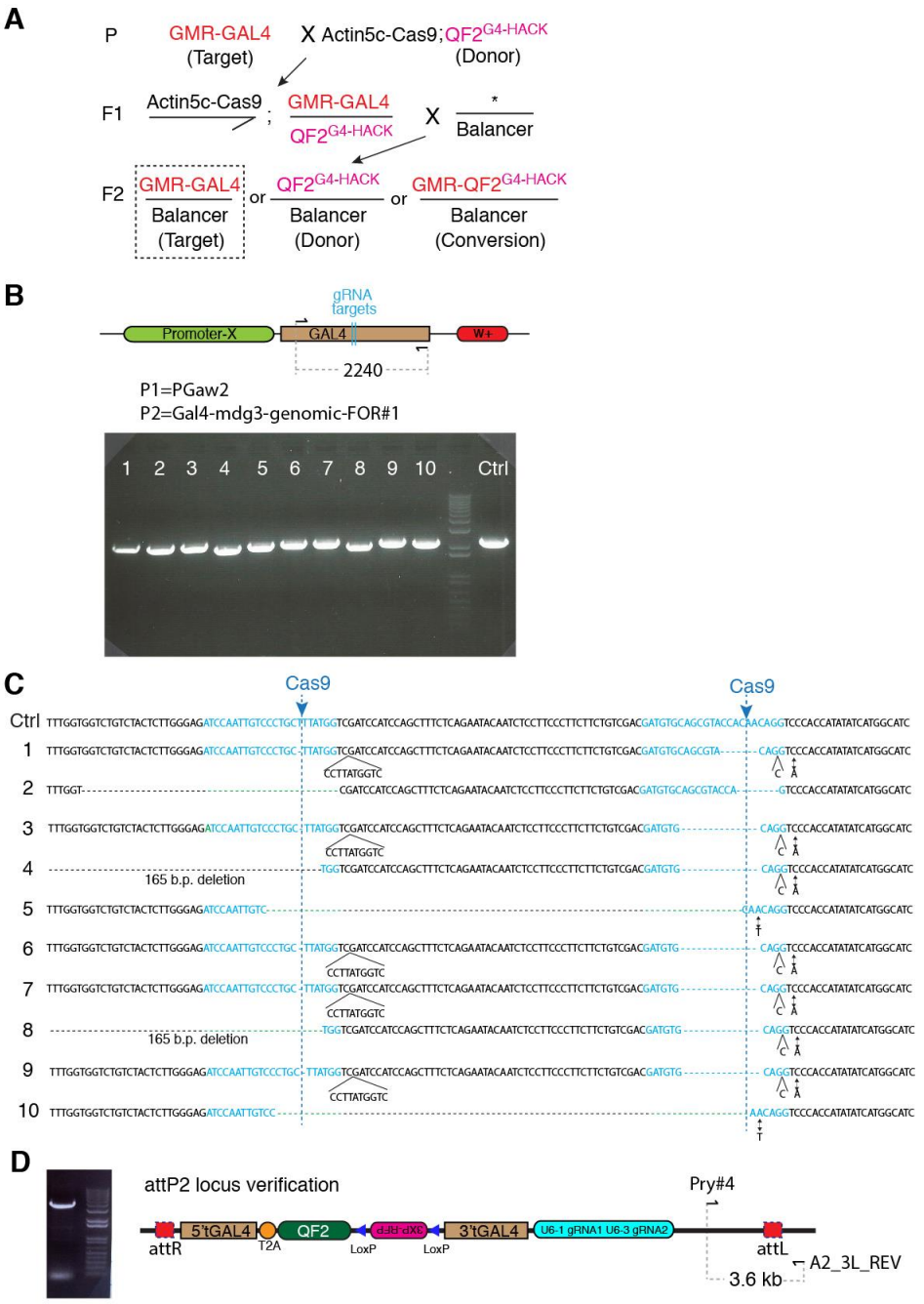

Figure S7: Low conversion rate at attP2 site is not due to inefficient DSB by CRISPR/Cas9. (**A**) Crossing scheme of *GMR-GAL4* and Donor *QF2^{G4H}* at the attp2 site. Unsuccessfully HACKed flies were selected for single fly genotyping (dashed-lined box) (**B**) PCR amplification of the *GAL4* DNA domain showed various sizes as compared to the control intact *GAL4* region. (**C**) DNA sequencing of the PCR results verified that all randomly selected unsuccessfully HACKed flies exhibited various degrees of indel mutations, confirming efficient DSB created by CRISPR/Cas9 (N=10). (**D**) Genomic PCR amplification verified that the *attP2 QF2^{G4H}* HACK donor is at the *attP2* site. A schematic of the primer locations in an attP2-integrated *attB-QF2^{G4H}* genomic region is shown.

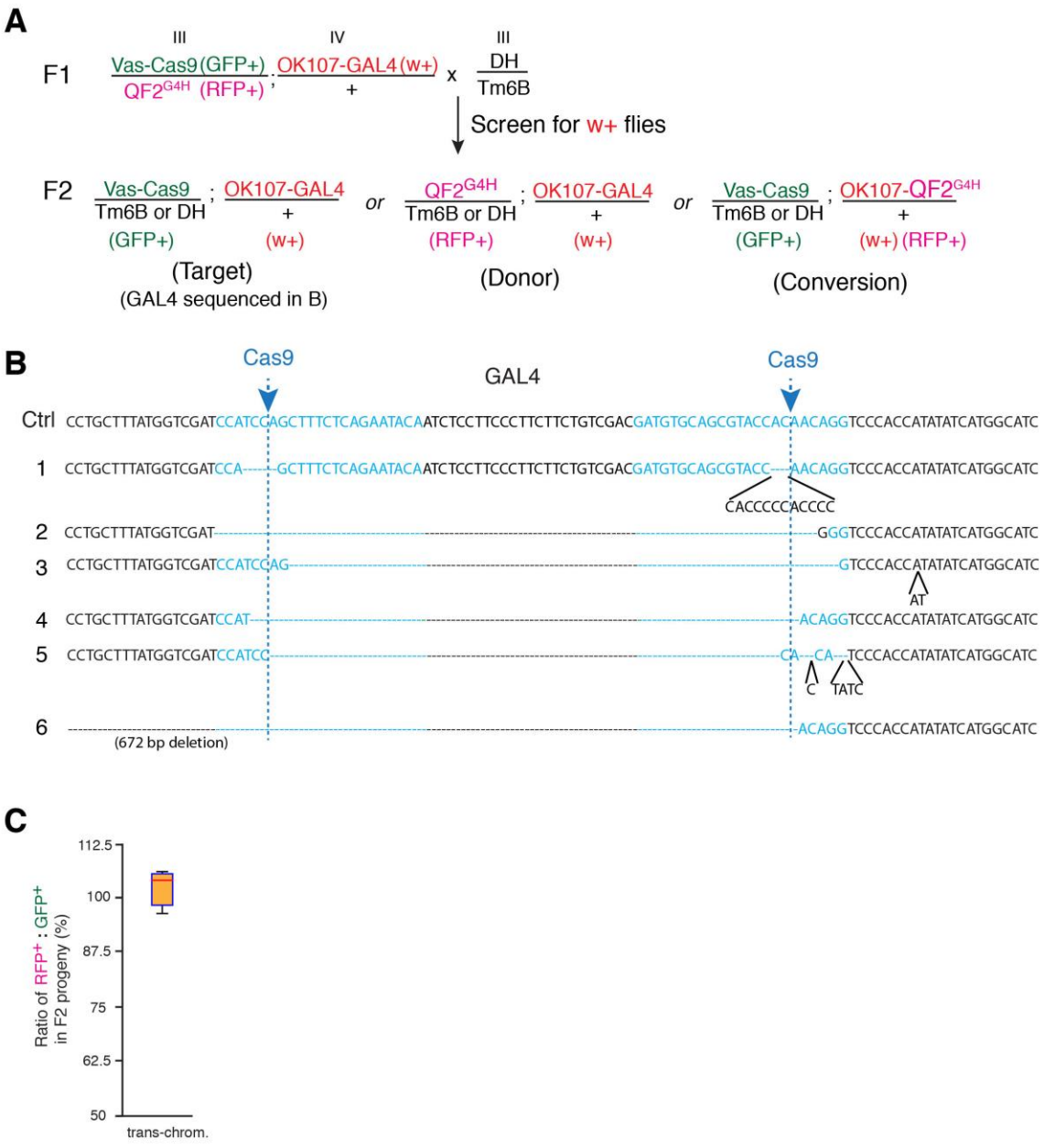

Figure S8: Single male genomic sequencing of unsuccessful trans-chromosomal HACK flies. (**A**) Crossing scheme of HACK *QF2^{G4H}* Donor on 3rd chromosome and *GAL4* on 4th chromosome (*OK107-GAL4*). (**B**) All of the flies showed different patterns of indel mutations at the gRNA target sites (N=6, 3 flies from HACK *QF2^{G4H}* Donor 70F4 and 3 flies from 64B5). The results confirm efficient DSB mediated by CRISPR/Cas9. (**C**) Non-*GAL4* 3rd chromosomes did not demonstrate a fitness cost due to gRNA and Cas9 expression, as calculated by the ratio of RFP+ (*QF2^{G4H}* Donor) to GFP+ (*Vas-Cas9*) F_2 animals from the cross shown in (**A**).

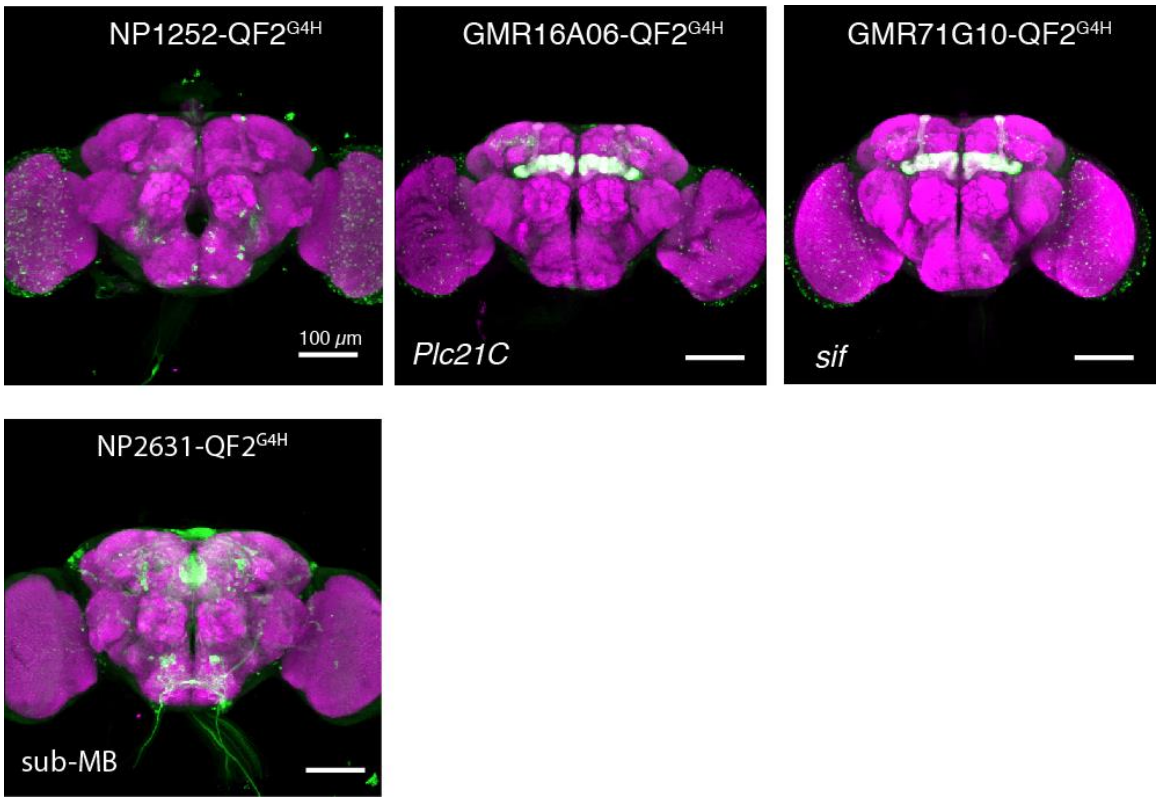

Figure S9: Expression patterns of *NP2631-QF2^{G4H}*, *NP1252-QF2^{G4H}*, *GMR16A06-QF2^{G4H}* and *GMR71G10-QF2^{G4H}*. Confocal images of representative brains stained for GFP (rabbit anti-GFP or chicken anti-GFP, see Methods for details). Reporters were 10x*QUAS-6xGFP*. Scale bar, 100 µm.

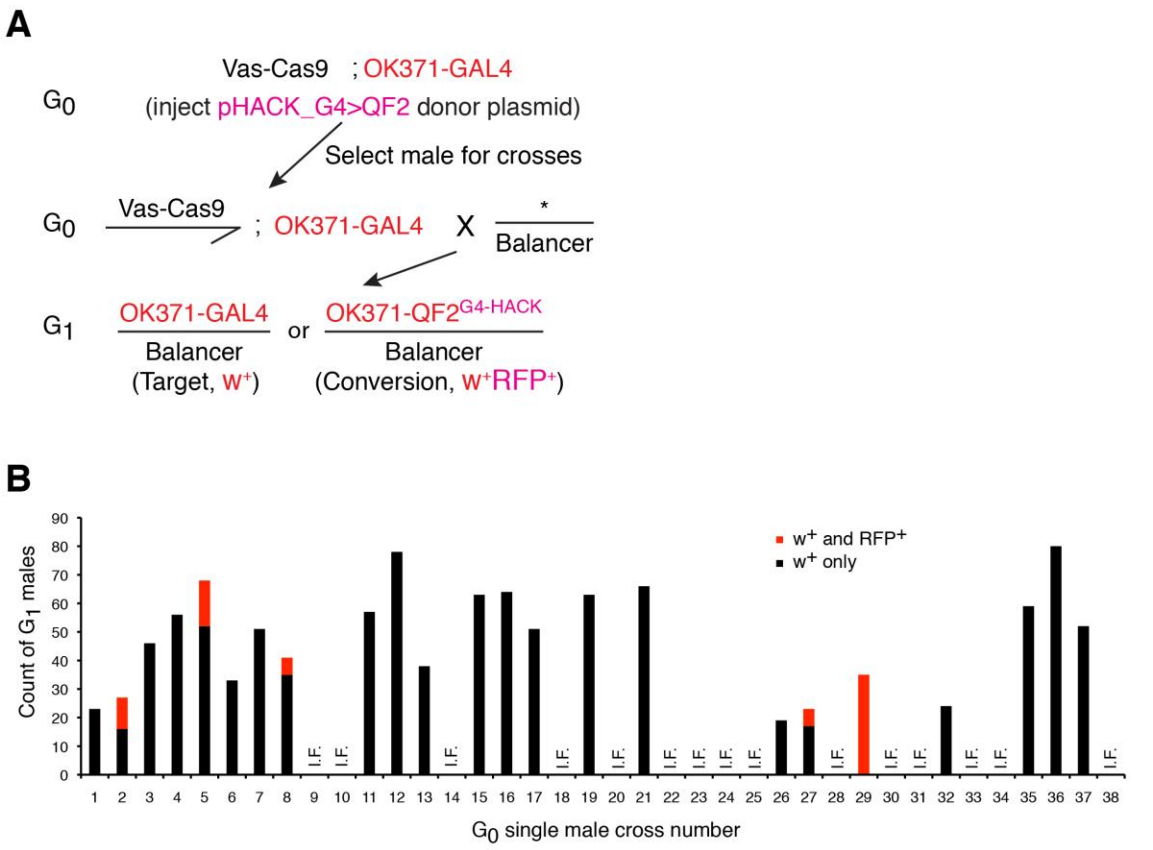

Figure S10: HACKing can be achieved by injection of donor DNA into target embryos (**A**) Example scheme for embryo injection of a HACK donor plasmid to convert the *OK371-GAL4* strain. The *pHACK_G4>QF2* construct provides the gRNAs and donor DNA for HDR. *Vas-Cas9* provides Cas9 expression in the germline. (**B**) Phenotypes of all male progeny from single male crosses from the injected animals. 5/23 fertile G_0 crosses produced G_1 progeny that had been HACKed. The success rate was 5.8 % (64 w^+RFP^+ G_1 males / 1107 total w^+ G_1 males). I.F., Infertile.

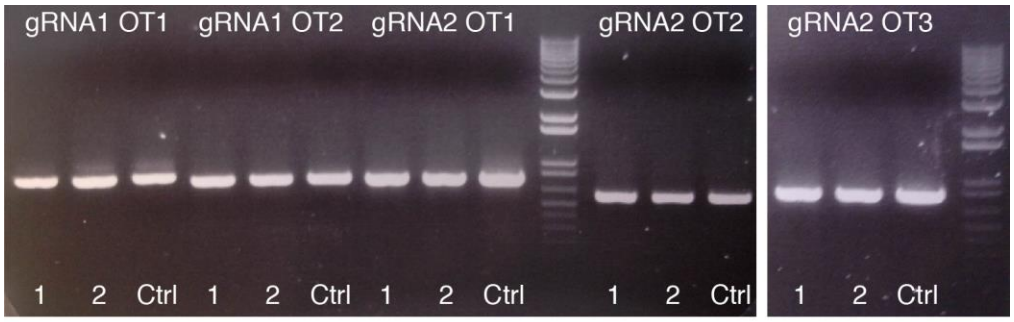

1: Act5C-Cas9; $QF2^{G4\text{-}HACK}$ (57C1)
2: Act5C-Cas9; ;$QF2^{G4\text{-}HACK}$ (70F4)
Ctrl: Act5C-Cas9

Figure S11: No indel mutations were found in off-targets predicted by a "maximum stringency" algorithm. The genomic region of predicted off target (OT) sites were PCR amplified from fly stocks containing Cas9 and *$QF2^{G4H}$* gRNAs. The size of the PCR products from two different stocks (1 and 2) and control (Ctrl) flies were similar.